

Article

Discovery of New Monocarbonyl Ligustrazine-Curcumin Hybrids for Intervention of Drug-Sensitive and Drug-Resistant Lung Cancer

Yong Ai, Bin Zhu, Caiping Ren, Fenghua Kang, Jinlong Li, Zhangjian Huang, Yisheng Lai, Sixun Peng, Ke Ding, Jide Tian, and Yihua Zhang

J. Med. Chem., **Just Accepted Manuscript** • DOI: 10.1021/acs.jmedchem.5b01203 • Publication Date (Web): 18 Feb 2016

Downloaded from <http://pubs.acs.org> on February 19, 2016

Just Accepted

“Just Accepted” manuscripts have been peer-reviewed and accepted for publication. They are posted online prior to technical editing, formatting for publication and author proofing. The American Chemical Society provides “Just Accepted” as a free service to the research community to expedite the dissemination of scientific material as soon as possible after acceptance. “Just Accepted” manuscripts appear in full in PDF format accompanied by an HTML abstract. “Just Accepted” manuscripts have been fully peer reviewed, but should not be considered the official version of record. They are accessible to all readers and citable by the Digital Object Identifier (DOI®). “Just Accepted” is an optional service offered to authors. Therefore, the “Just Accepted” Web site may not include all articles that will be published in the journal. After a manuscript is technically edited and formatted, it will be removed from the “Just Accepted” Web site and published as an ASAP article. Note that technical editing may introduce minor changes to the manuscript text and/or graphics which could affect content, and all legal disclaimers and ethical guidelines that apply to the journal pertain. ACS cannot be held responsible for errors or consequences arising from the use of information contained in these “Just Accepted” manuscripts.

1
2
3
4 **Discovery of New Monocarbonyl Ligustrazine-Curcumin Hybrids**
5
6
7 **for Intervention of Drug-Sensitive and Drug-Resistant Lung**
8
9 **Cancer**
10
11
12
13
14
15
16

17 Yong Ai,^{‡a,b} Bin Zhu,^{‡c} Caiping Ren,^{*c} Fenghua Kang,^{a,b} Jinlong Li,^c Zhangjian
18 Huang,^{*a,b} Yisheng Lai,^{a,b} Sixun Peng,^{a,b} Ke Ding,^d Jide Tian,^e and Yihua Zhang^{*a,b}
19
20
21
22
23
24

25 ^aState Key Laboratory of Natural Medicines, China Pharmaceutical University, Nanjing
26 210009, PR China
27

28 ^bJiangsu Key Laboratory of Drug Discovery for Metabolic Diseases, China
29 Pharmaceutical University, Nanjing 210009, PR China
30
31
32
33

34 ^cCancer Research Institute, Collaborative Innovation Center for Cancer Medicine, Key
35 Laboratory for Carcinogenesis of Chinese Ministry of Health, School of Basic Medical
36 Sciences, Central South University, Changsha 410078, PR China
37
38
39
40
41
42

43 ^dKey Laboratory of Regenerative Biology and Institute of Chemical Biology, Guangzhou
44 Institutes of Biomedicine and Health, Chinese Academy of Sciences, Guangzhou 510530,
45 PR China
46
47
48
49
50

51 ^eDepartment of Molecular and Medical Pharmacology, University of California, Los
52 Angeles, California 90095, United States
53
54
55
56
57
58
59
60

1
2
3 **ABSTRACT** The elevation of oxidative stress preferentially in cancer cells by inhibiting
4
5 thioredoxin reductase (TrxR) and/or enhancing reactive oxygen species (ROS) production
6
7
8 has emerged as an effective strategy for selectively targeting cancer cells. In this study,
9
10 we designed and synthesized twenty-one ligustrazine-curcumin hybrids (**10a-u**).
11
12 Biological evaluation indicated that the most active compound **10d** significantly inhibited
13
14 the proliferation of drug-sensitive (A549, SPC-A-1, LTEP-G-2) and drug-resistant
15
16 (A549/DDP) lung cancer cells but had little effect on non-tumor lung epithelial-like cells
17
18 (HBE). Furthermore, **10d** suppressed the TrxR/Trx system and promoted intracellular
19
20 ROS accumulation and cancer cell apoptosis. Additionally, **10d** inhibited the NF- κ B,
21
22 AKT and ERK signaling, P-gp-mediated efflux of rhodamine 123, P-gp ATPase activity
23
24 and P-gp expression in A549/DDP cells. Finally, **10d** repressed the growth of implanted
25
26 human drug-resistant lung cancer in mice. Together, **10d** acts a novel TrxR inhibitor and
27
28 may be a promising candidate for intervention of lung cancer.
29
30
31
32
33
34
35
36
37
38
39
40
41
42
43
44
45
46
47
48
49
50
51
52
53
54
55
56
57
58
59
60

INTRODUCTION

Cancer cells are usually exposed to a moderate level of reactive oxygen species (ROS), primarily due to their active metabolism in response to oncogenic signals.¹ In fact, cancer cells take advantage of this moderate oxidative stress for several important processes such as proliferation, angiogenesis, and metastasis.² However, high levels of ROS irreversibly damage DNA and lipids, and ultimately cause cancer cell apoptosis.³ Recently, pharmacological elevation of intracellular ROS has emerged as an effective strategy for selectively targeting cancer cells. While an exogenous ROS insult is tolerable to normal cells it may exceed the threshold cancer cells can endure and lead to selective cytotoxicity against cancer cells.^{4,5} Actually, there have been increasing efforts to increase the levels of ROS specifically in cancer cells for 'oxidation therapy'.⁶⁻⁸ One strategy for oxidation therapy is to directly deliver ROS promoting agents such as ligustrazine (**1**, Figure 1),⁹ arsenic trioxide (As_2O_3)^{10,11} and glucose oxidase to tumor tissues.^{12,13}

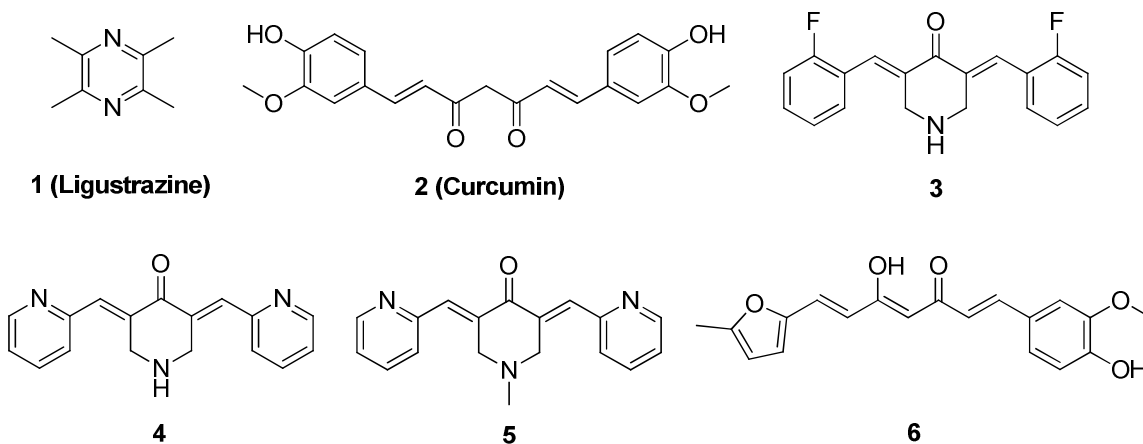


Figure 1. Chemical structures of ligustrazine, curcumin and SCAs.

1
2
3
4
5
6
7
8
9
10
11
12
13
14
15
16
17
18
19
20
21
22
23
24
25
26
Ligustrazine is a Chinese medicine for treatment of cardiovascular and cerebrovascular diseases.¹⁴ Recently, ligustrazine has been shown to increase intracellular ROS accumulation, and to induce cancer cell apoptosis.^{9,15,16} More importantly, ligustrazine is a reversal agent against ATP-binding cassette (ABC) transporter-mediated multidrug resistance (MDR).^{17,18} Unfortunately, ligustrazine has a short half-life and low bioavailability in vivo and is required for frequent treatments with a high dose, which results in the drug-accumulation related toxicity.¹⁹ Besides, ligustrazine is usually used in combination with an anticancer drug to circumvent MDR, which may lead to pharmacokinetic interactions of the drugs and to increase adverse effects of the anticancer therapy. Thus, modification of ligustrazine is needed to improve its therapeutic potency.

27
28
29
30
31
32
33
34
35
36
37
38
39
40
41
42
43
44
45
46
47
48
49
50
51
52
53
54
55
56
57
58
59
60
'Oxidation therapy' is to disrupt the redox balance in cancer cells by suppressing the antioxidant systems.^{6,20-22} The thioredoxin system, one of the key antioxidant systems is composed of thioredoxin reductase (TrxR), thioredoxin (Trx), and NADPH, and regulates numerous cellular signal pathways involved in cell survival and proliferation.²³⁻²⁵ TrxR is the only known physiological enzyme to catalyze the reduction of oxidized Trx. Importantly, the thioredoxin system is often overexpressed in many tumors,^{26,27} associated with chemoresistance of cancers.²⁸ Recently, accumulating data support that TrxR is a promising target for development of novel anticancer agents, and the efficacy of this redox-modulating method has been demonstrated in models of drug-resistant cancers.²⁹ In the past years, a great endeavor has been witnessed in discovering and developing a variety of TrxR-targeting small molecules, including curcumin (**2**, Figure 1), cinnamaldehydes, acylfulvenes, flavonoids, etc., many of which have been combined with an anticancer drug as a potential therapy against drug-sensitive and drug-resistant

1
2
3 cancers.³⁰⁻³⁷
4
5

6 Curcumin, a yellow spice extracted from the *Curcuma longa*, has been identified as a
7 TrxR inhibitor with anticancer activity.³⁸⁻⁴¹ To improve its potency, many synthetic
8 curcumin analogs (SCAs) have been prepared, including EF24 (**3**), EF31 (**4**), UBS109 (**5**)
9 (Figure 1),⁴² **6**, and others.^{43,44} Among them, those monocarbonyl curcumin analogs
10 display strong anticancer activity by inhibiting cancer cell proliferation and inducing
11 cancer cell apoptosis.⁴⁵⁻⁵⁰
12
13
14
15
16
17
18

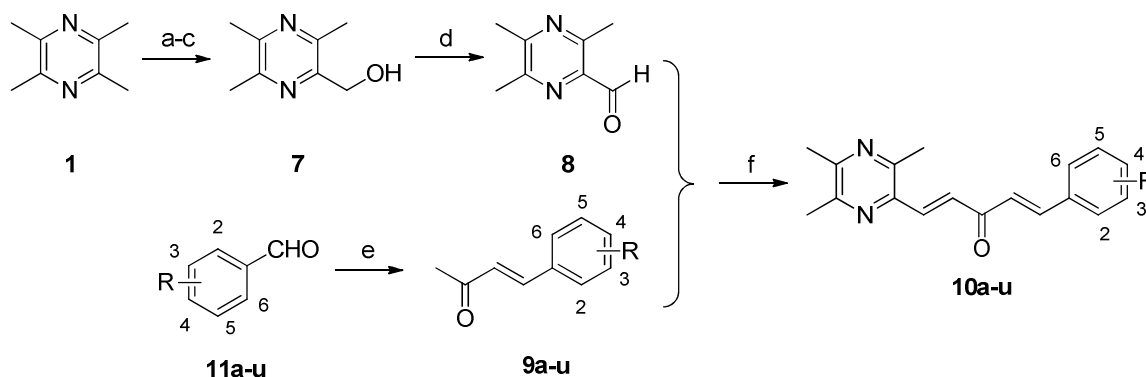
19 Given that use of an ROS promoting agent together with an inhibitor of ROS
20 scavenging can amplify oxidative stress and be effective for treatment of advanced solid
21 tumors,^{21,51} we hypothesized that new hybrids of ligustrazine scaffold with curcumin
22 moiety might not only elevate ROS production but also diminish the antioxidant defense
23 systems, leading to ROS accumulation preferentially in cancer cells and to subsequent
24 ROS-mediated cytotoxicity against cancer cells. Accordingly, we synthesized hybrids
25 **10a-u** by substituting one of the two aromatic rings of curcumin analogs with ligustrazine
26 via a Claisen-Schmidt condensation reaction, and evaluated their bioactivity in vitro and
27 in vivo.
28
29
30
31
32
33
34
35
36
37
38
39
40
41
42
43
44

45 RESULTS AND DISCUSSION

46
47 **Chemistry.** The synthetic routes to compounds **10a-u** are depicted in Scheme 1.
48 2-Hydroxymethyl-3,5,6-trimethylpyrazine **7** was prepared by the Boekelheide reaction
49 starting from ligustrazine **1** as described previously.⁵² The generated **7** underwent a
50 2-iodoxybenzoic acid (IBX) oxidation giving the aldehyde group-containing intermediate
51 **8**, which was directly reacted with the aryl-substituted enones **9a-u**, prepared from
52
53
54
55
56
57
58
59
60

corresponding aldehydes **11a-u**,⁵³ in the presence of borontrifluoride-etherate (BF₃·Et₂O) via a Claisen-Schmidt condensation reaction to get the target compounds **10a-u**. The purity of all hybrids was greater than 95% and determined by HPLC analysis. The structures of all hybrids were fully characterized and identified as *E,E* configuration.

Scheme 1. Synthetic Routes of Ligustrazine-Curcumin Hybrids **10a-u**.^a



9-11a R = 2-OH	9-11h R = 4-OCH ₃	9-11m R = H	9-11t R = 4-NO ₂
9-11b R = 3-OH	9-11i R = 3,4-dimethoxy	9-11n R = 4-F	9-11u R =
9-11c R = 4-OH	9-11j R = 2,4-dimethoxy	9-11o R = 4-Cl	
9-11d R = 3-OCH ₃ -4-OH	9-11k R = 3,4,5-trimethoxy	9-11p R = 4-CF ₃	
9-11e R = 2-OH-3-OCH ₃	9-11l R =	9-11q R = 4-CH ₃	
9-11f R = 2-OCH ₃		9-11r R = 2-NO ₂	
9-11g R = 3-OCH ₃		9-11s R = 3-NO ₂	

^aReagents and conditions: (a) 30% H₂O₂, acetic acid, 70 °C, 8 h.; (b) acetic anhydride, reflux, 2 h; (c) 20% NaOH; (d) IBX, DMSO, room temperature, 0.5 h; (e) Morpholinium trifluoroacetate, acetone, 60 °C, sealing tube reaction for 24 h; (f) BF₃·Et₂O, 1,4-dioxane, reflux, 4-6 h.

BIOLOGICAL EVALUATION

Evaluation of Antiproliferative Activity. Given that compounds **10a-u** we designed may effectively target TrxR expressed in cancer cells, we first examined the levels of

TrxR expression in drug-sensitive human lung cancer A549, drug-resistant human lung cancer A549/DDP cells and human non-tumor bronchial epithelial HBE cells by Western blot assay. We observed that the levels of TrxR expression in A549 cells were significantly higher than that in HBE cells, but significantly lower than that in A549/DDP cells ($P < 0.001$). Hence, TrxR was up-regulated in lung cancer cells, particularly in drug-resistant A549/DDP cells.

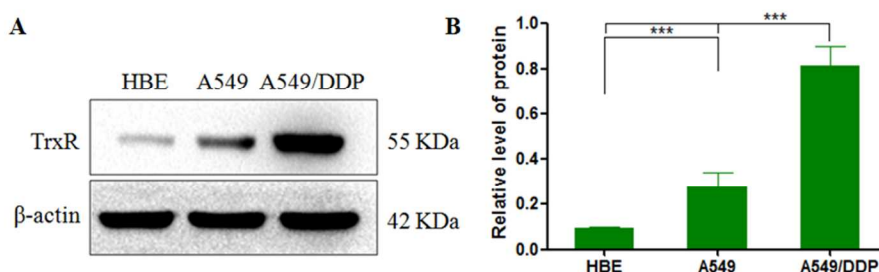


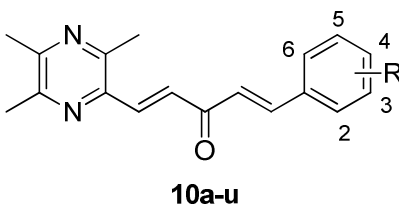
Figure 2. TrxR Expression in HBE, A549 and A549/DDP cells. HBE, A549 and A549/DDP cells were harvested and lysed. The relative levels of TrxR to control β -actin in HBE, A549 and A549/DDP cell lysates were determined by Western blot. Data are representative of three independent experiments. *** $P < 0.001$.

Next, the antiproliferative activity of compounds **10a-u** against A549 and A549/DDP cells was initially screened by the MTT assay using cisplatin (DDP) as a positive control. As shown in Table 1, compounds **10a-l** and **10q** displayed potent inhibitory activity against both A549 ($IC_{50} = 1.16-4.78 \mu M$) and A549/DDP ($IC_{50} = 0.60-5.20 \mu M$) cell viability, and their anti-proliferative activity was more potent than DDP ($IC_{50} = 8.10$ and $45.14 \mu M$) their individual moieties, **1** ($IC_{50} > 200$ and $200 \mu M$) and **2** ($IC_{50} = 38.12$ and $32.39 \mu M$), and even the combination of **1** and **2** ($IC_{50} = 24.33$ and $25.17 \mu M$). It was

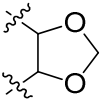
obvious that R substitutes at benzene ring of the hybrids (Table 1) may be crucial for their anticancer activity. In general, the compounds with an electron-donating group such as methoxy, hydroxy or methyl at benzene ring (**10a-l** and **10q**) usually showed more potent inhibitory activity than those bearing an electron-withdrawing group such as halogen, trifluoromethyl, nitro or benzene (**10n-p** and **10r-u**).

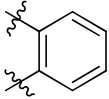
Subsequently, the five potent compounds (**10d**, **10e**, and **10i-k**) were further investigated for their antitumor efficacy by MTT (Table 2). We found that all of the five compounds displayed more potent activity ($IC_{50} = 2.34-6.32 \mu M$) than DDP ($IC_{50} = 14.18-15.51 \mu M$) against human lung cancer SPC-A-1 and LTEP-G-2 cells that were similar to A549 cells with high levels of TrxR expression. While DDP had similar inhibitory activity against both lung cancer and non-tumor HBE cells, **10d** exhibited a 7~35-fold less antiproliferative activity against HBE cells ($IC_{50} = 21.34 \mu M$), suggesting that **10d** may have antiproliferative activity selectively against cancer cells.

Table 1. The antiproliferative activity of target compounds (**10a-u**) against human lung cancer A549 and A549/DDP cells.



Compd	R substituents	$IC_{50} (\mu M)^a$
-------	----------------	---------------------

	2	3	4	5	A549	A549/DDP
10a	OH	H	H	H	4.78 ± 0.35 ^b	3.90 ± 0.14 ^b
10b	H	OH	H	H	4.30 ± 0.32 ^b	3.70 ± 0.21 ^b
10c	H	H	OH	H	4.01 ± 0.53 ^b	4.79 ± 0.77 ^b
10d	H	OCH ₃	OH	H	2.19 ± 0.14 ^b	0.60 ± 0.11 ^b
10e	OH	OCH ₃	H	H	2.85 ± 0.22 ^b	2.19 ± 0.15 ^b
10f	OCH ₃	H	H	H	3.20 ± 0.69 ^b	4.74 ± 0.41 ^b
10g	H	OCH ₃	H	H	3.30 ± 0.12 ^b	3.44 ± 0.24 ^b
10h	H	H	OCH ₃	H	3.50 ± 0.89 ^b	3.61 ± 0.77 ^b
10i	H	OCH ₃	OCH ₃	H	3.79 ± 0.22 ^b	2.44 ± 0.24 ^b
10j	OCH ₃	H	OCH ₃	H	3.07 ± 1.55 ^b	2.85 ± 0.55 ^b
10k	H	OCH ₃	OCH ₃	OCH ₃	1.60 ± 0.11 ^b	1.00 ± 0.13 ^b
10l	H			H	4.50 ± 0.54 ^b	5.20 ± 0.97 ^b
10m	H	H	H	H	12.31 ± 1.11	11.88 ± 0.66 ^b
10n	H	H	F	H	5.90 ± 0.47	7.44 ± 0.59 ^b
10o	H	H	Cl	H	15.8 ± 1.23	7.49 ± 0.67 ^b
10p	H	H	CF ₃	H	11.7 ± 1.09	6.90 ± 0.53 ^b
10q	H	H	CH ₃	H	4.3 ± 1.29 ^b	3.99 ± 0.33 ^b
10r	NO ₂	H	H	H	17.33 ± 0.54	6.39 ± 0.21 ^b
10s	H	NO ₂	H	H	6.70 ± 0.14	6.69 ± 0.11 ^b

10t	H	H	NO ₂	H	9.60 ± 0.97	7.90 ± 0.17 ^b
10u	H			H	7.10 ± 0.74	11.80 ± 0.91 ^b
1					> 200	> 200
2					38.12 ± 2.87	32.39 ± 3.14
1+2					24.33 ± 2.77	25.17 ± 2.89
DDP					8.10 ± 0.97	45.14 ± 2.11

^aCells were treated in triplicate with tested compounds for 72 h and the cell viability was determined using MTT assay. ^b*P* < 0.01 vs the DDP.

Table 2. The antiproliferative activity of selected compounds against human lung cancer SPC-A-1, LTEP-G-2 and non-tumor HBE cells.

Compd	IC ₅₀ (μM) ^a		
	SPC-A-1	LTEP-G-2	HBE
10d	3.12 ± 0.41 ^b	2.88 ± 0.13 ^b	21.34 ± 3.76 ^b
10e	5.71 ± 0.47 ^b	5.01 ± 0.34 ^b	17.56 ± 1.55 ^b
10i	5.42 ± 0.38 ^b	4.36 ± 0.23 ^b	16.23 ± 2.68 ^b
10j	6.32 ± 0.59 ^b	5.91 ± 0.45 ^b	20.76 ± 1.55 ^b
10k	5.35 ± 0.44 ^b	2.34 ± 0.13 ^b	14.35 ± 1.37
DDP	15.51 ± 1.23	14.18 ± 1.24	10.37 ± 1.54

1
2
3
4
5
6
7
8
9
10
11
12
13
14
15
16
17
18
19
20
21
22
23
24
25
26
27
28
29
30
31
32
33
34
35
36
37
38
39
40
41
42
43
44
45
46
47
48
49
50
51
52
53
54
55
56
57
58
59
60

^aCells were treated in triplicate with tested compounds for 72 h and the cell viability was determined using MTT assay. ^b*P* < 0.01 vs the DDP.

Inhibition of TrxR by selected compounds in both cell-free and cellular assay. Since **10d**, **10e**, and **10i-k** displayed the promising antiproliferative activity against lung cancer cells, we tested their TrxR inhibitory activity in purified TrxR enzyme and in A549 and A549/DDP cells. Firstly, the TrxR inhibitory activity of **10d**, **10e**, and **10i-k** in purified TrxR enzyme was determined with DTNB assay.³⁷ As shown in Table 3, **10d**, **10e**, and **10i-k** exhibited more potent TrxR inhibitory activity ($IC_{50} = 2.95-7.63 \mu M$) than curcumin **2** ($IC_{50} = 41.42 \pm 3.21 \mu M$), while ligustrazine **1** showed little TrxR inhibitory activity at 200 μM . Next, we determined the TrxR inhibitory activity of **10d**, **10e**, and **10i-k** in cells. Briefly, A549 and A549/DDP cells were treated with different concentrations of each compound for 24 h. The activity of TrxR in different groups of cells was determined using a Thioredoxin Reductase Assay Kit (Cayman).⁵⁴ As shown in Table 3, all of the five compounds exerted potent TrxR inhibitory activity ($IC_{50} = 1.22-4.73 \mu M$). As expected, **10d** showed the highest TrxR inhibitory activity, which was ~32-fold more potent than curcumin **2** (IC_{50} s = 40.56, 39.42 μM), suggesting that **10d** may be a novel TrxR inhibitor for further investigation.

Furthermore, we determined the impact of **10d** treatment on the expression of TrxR and Trx in A549 and A549/DDP cells by Western blot. As shown in Figure 3, **10d**

significantly reduced the relative levels of TrxR and Trx to GAPDH expression in A549 and A549/DDP cells. Hence, the decrease in the levels of TrxR and Trx expression by **10d** may contribute to its inhibition on TrxR and anticancer activity in lung cancer cells.

Table 3. Inhibition of compounds on TrxR activity in cell-free and cellular assays.

Compd	In cell-free assay	In cellular assay IC ₅₀ (μM) ^b	
	IC ₅₀ (μM) ^a	A549	A549/DDP
10d	2.95 ± 0.17 ^c	1.49 ± 0.11 ^c	1.22 ± 0.13 ^c
10e	5.30 ± 0.22 ^c	4.73 ± 0.37 ^c	4.64 ± 0.34 ^c
10i	7.09 ± 0.35 ^c	4.17 ± 0.24 ^c	4.22 ± 0.31 ^c
10j	7.63 ± 0.13 ^c	4.12 ± 0.2 ^c	4.26 ± 0.44 ^c
10k	3.06 ± 0.21 ^c	2.36 ± 0.21 ^c	1.98 ± 0.14 ^c
1	> 200	> 200	> 200
2	41.42 ± 3.21	40.56 ± 3.67	39.42 ± 2.11

^aThe TrxR inhibition activities in cell-free assay were measured by DTNB assay as described in the Experimental Section. ^bThe TrxR inhibitory activity of selected compounds in A549 and A549/DDP cells using a Thioredoxin Reductase Assay Kit (Cayman). ^c*P* < 0.05 vs the ligustrazine **1** and curcumin **2**.

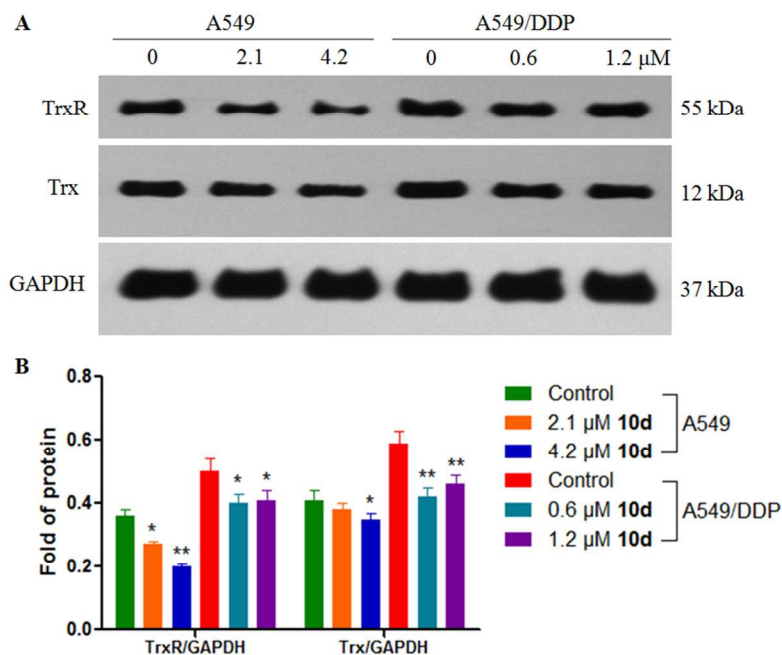


Figure 3. Effect of **10d** on the relative levels of TrxR and Trx expression in A549 and A549/DDP cells. Cells were treated with **10d** or vehicle for 24 h and the relative levels of TrxR and Trx to control GAPDH expression were determined by Western blot. Data are representative of three independent experiments. * $P < 0.05$, ** $P < 0.01$ vs the control.

Effect of 10d on the ROS Accumulation in cells. The Trx system is crucial for the intracellular redox balance to prevent excess ROS accumulation.^{34,54,55} The inhibition of TrxR and Trx may disturb the redox balance, leading to intracellular ROS accumulation in cancer cells. Accordingly, we examined the impact of **10d** on ROS levels in A549 and A549/DDP cells. A549 and A549/DDP cells were treated in triplicate with various concentrations of **10d**, **1**, and **2** for 60 min. The cells were collected longitudinally and stained with dihydroethidium (DHE, Beyotime). The levels of intracellular ROS were determined by measuring the fluorescent signals using a fluorescence microplate reader. As shown in Figure 4A and B, treatment with **10d** rapidly and significantly increased the

levels of intracellular ROS in both A549 and A549/DDP cells. More importantly, treatment with **10d** significantly reduced the viability of A549 and A549/DDP cells (Figure 4C), which was partially or completely abrogated by pre-treatment with 10 mM N-acetyl-L-cysteine (NAC) or glutathione (GSH), respectively. These data indicated that **10d** promoted ROS accumulation that was cytotoxic to lung cancer cells.

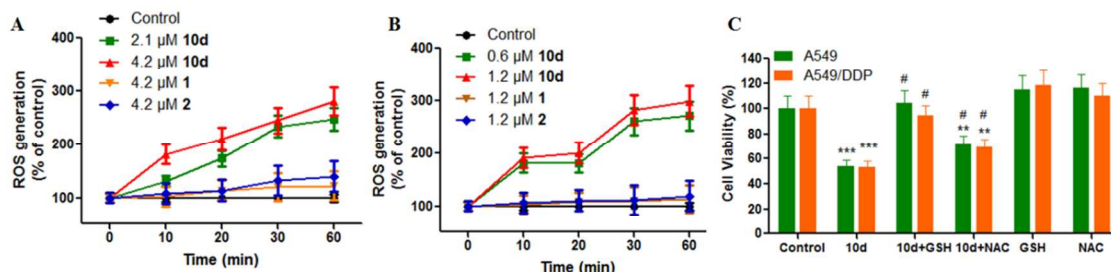


Figure 4. Treatment with **10d** induces the accumulation of toxic ROS in A549 (A) and A549/DDP (B) cells. (C) Pre-treatment with 10 mM GSH or NAC for 1 h demolishes the cytotoxicity of **10d** against A549 and A549/DDP cells. Data are representative of three independent experiments. $**P < 0.01$, $***P < 0.001$ vs the control. $^{\#}P < 0.05$ vs the **10d** group.

Induction of A549 and A549/DDP cell apoptosis. To determine whether the inhibitory effects of **10d** on lung cancer cellular proliferation are accompanied by enhanced cancer cell apoptosis, Annexin V-FITC and propidium iodide (PI) staining were carried out, and the percentages of apoptotic cells were tested using flow cytometry assay. A549 and A549/DDP cells were incubated with different concentrations of vehicle, **10d**, ligustrazine **1**, or curcumin **2** for 24 h. We observed that treatment with **10d** induced apoptosis in both A549 and A549/DDP cells (Figure 5), which were significantly stronger than that of **1** and **2**.

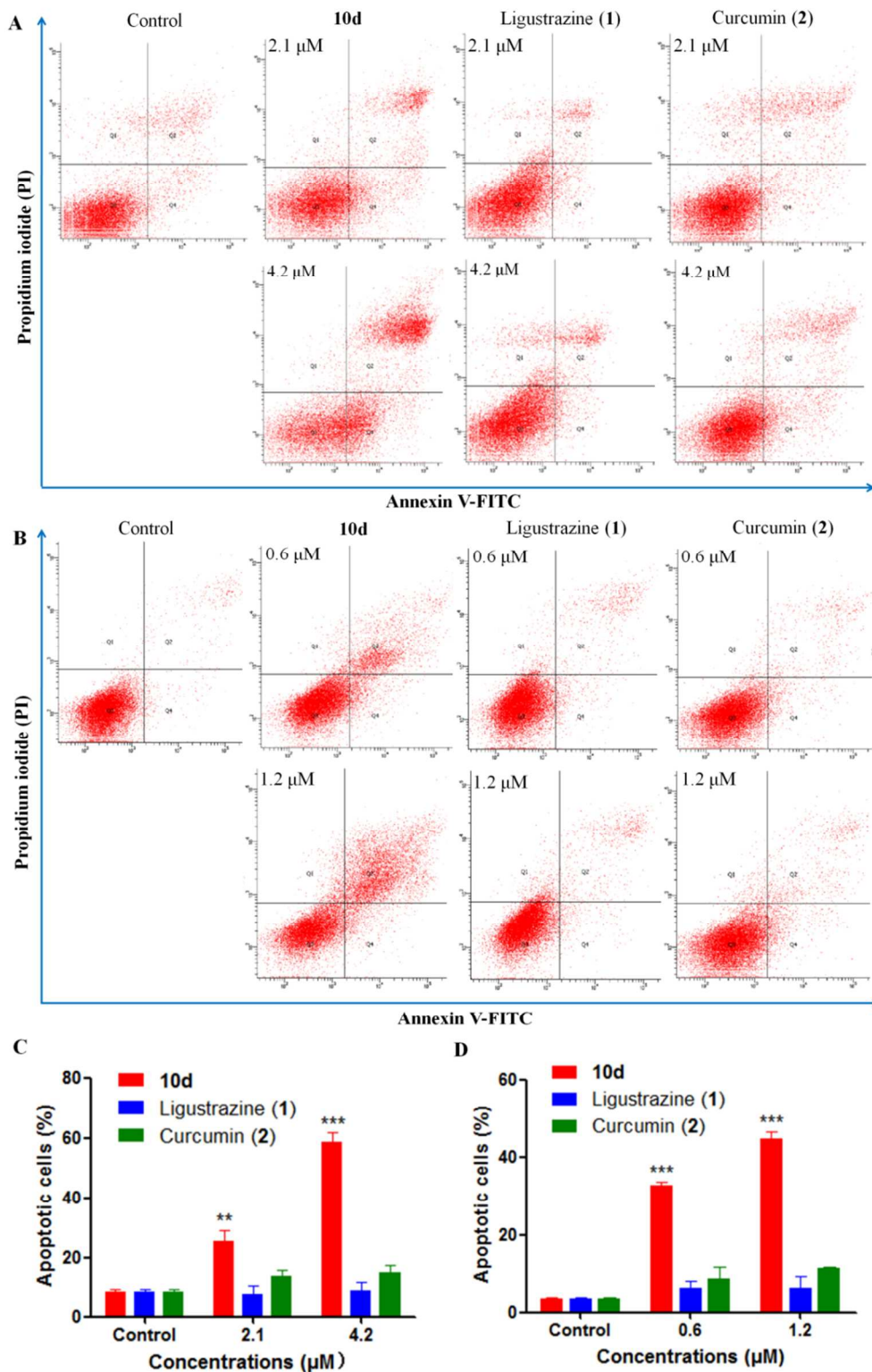


Figure 5. Apoptosis of A549 (A, C) and A549/DDP (B, D) cells treated with **10d**, ligustrazine **1** and curcumin **2** for 24 h. Values are the means \pm SD from at least three

independent experiments. $**P < 0.01$, $***P < 0.001$ vs the ligustrazine **1** and curcumin **2** groups.

Furthermore, Western blot assay revealed that treatment with **10d** dramatically decreased the levels of anti-apoptotic Bcl-2, but increased the levels of pro-apoptotic Bax expression in A549 and A549/DDP cells (Figure 6A). Quantitative analysis revealed that treatment with **10d** significantly increased the ratios of Bax to Bcl-2 (Figure 6B). Caspase activation is a critical event in the initiation and execution of apoptosis in cells. Treatment with **10d** also significantly increased the relative levels of cleaved caspase 3 and poly(ADP-ribose)polymerase (PARP) in A549 and A549/DDP cells.

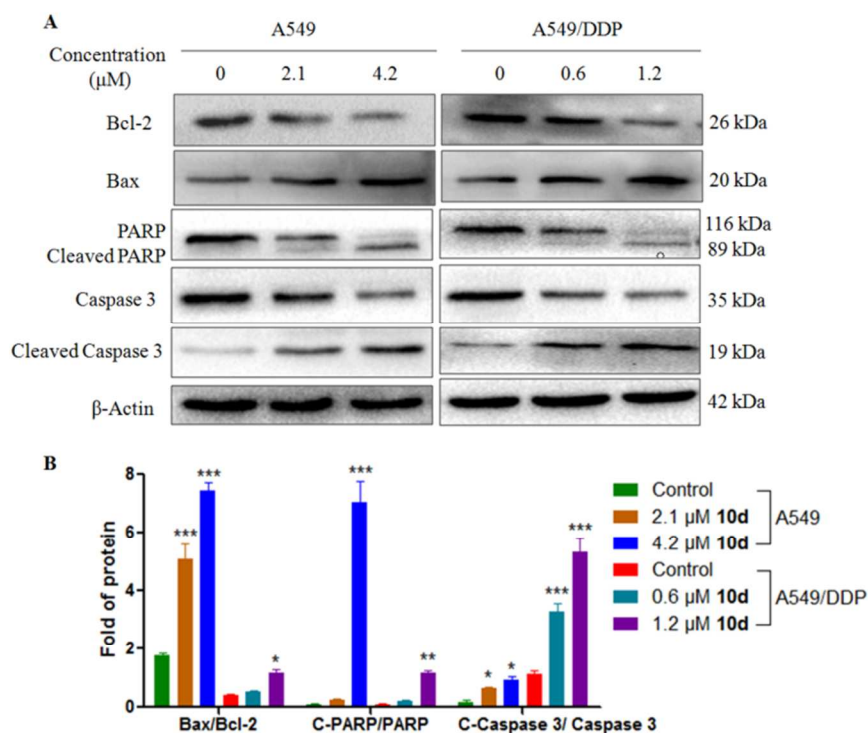


Figure 6. Effect of **10d** on the relative levels of Bcl-2, Bax, PARP, and Caspase 3 expression in A549 and A549/DDP cells. Cells were treated with **10d** (A549, 2.1 μM or

1
2
3 4.2 μM ; A549/DDP, 0.6 μM or 1.2 μM) or vehicle for 24 h and the relative protein levels
4
5 of Bcl-2, Bax, PARP, and Caspase 3 to β -actin were determined using Western blot
6
7 assays. Data are representative of three independent experiments. * $P < 0.05$, ** $P < 0.01$,
8
9 *** $P < 0.001$ vs the control.
10
11

12
13
14
15 **Effects of 10d on the NF- κ B, AKT, and ERK Signaling.** Recent studies indicate that
16
17 high levels of ROS in cancer cells directly inhibit the NF- κ B, AKT and ERK
18
19 activation,⁵⁵⁻⁵⁷ and aberrant activation of NF- κ B, AKT and ERK are associated with the
20
21 proliferation and drug resistance of tumor cells.⁵⁸⁻⁶³ To further understand the molecular
22
23 mechanisms underlying the activity of **10d**, we investigated the regulatory effects of **10d**
24
25 on the NF- κ B, AKT, and ERK signaling in A549 and A549/DDP cells. The cells were
26
27 treated with various concentrations of **10d**. The levels of NF- κ B, AKT, and ERK
28
29 expression and phosphorylation were determined using Western blotting. Although
30
31 treatment with **10d** did not alter the levels of NF- κ B and ERK expression, it significantly
32
33 suppressed the phosphorylations of NF- κ B, AKT and ERK in A549 and A549/DDP cells
34
35 (Figure 7). These results suggest that **10d** may inhibit spontaneous activation of the
36
37 NF- κ B, AKT, and ERK pathways, contributing to its antitumor activity in lung cancer
38
39 cells. Nevertheless, the precise mechanisms underlying the action of **10d** remain to be
40
41 further investigated.
42
43
44
45
46
47
48
49
50
51
52
53
54
55
56
57
58
59
60

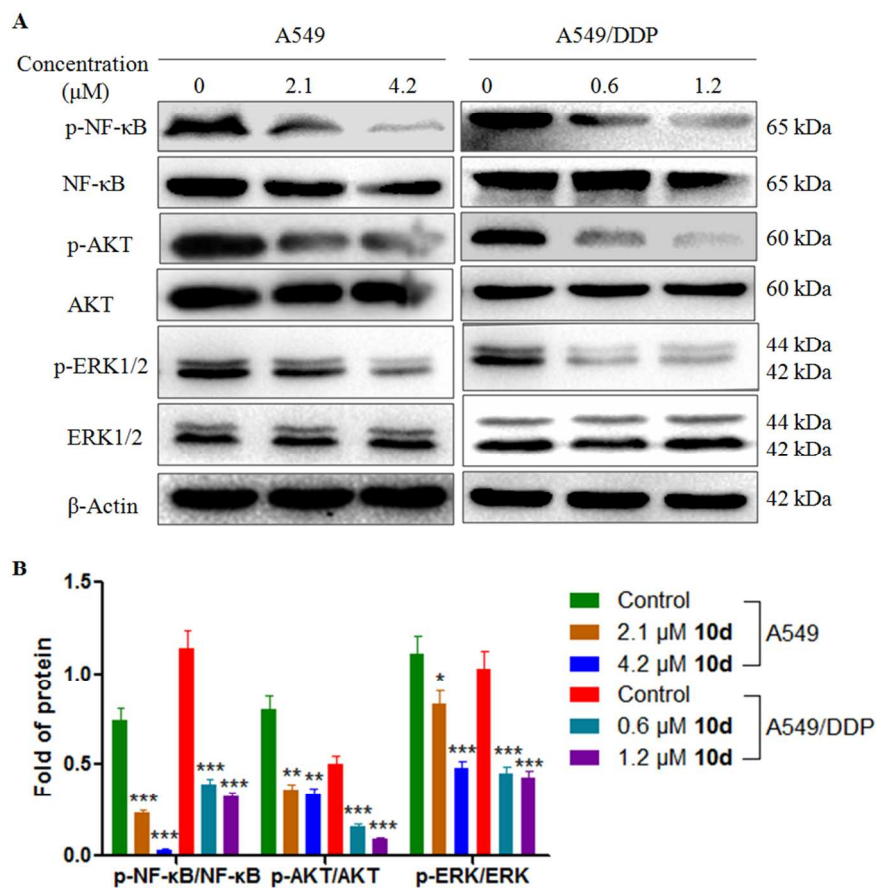


Figure 7. Effect of **10d** on the NF-κB, AKT and ERK signaling in A549 and A549/DDP cells. Cells were treated with **10d** (A549, 2.1 μM or 4.2 μM; A549/DDP, 0.6 μM or 1.2 μM) or vehicle for 24 h and the relative levels of NF-κB, AKT and ERK expression and phosphorylation were determined using Western blot assays. Data are representative of three independent experiments. * $P < 0.05$, ** $P < 0.01$, *** $P < 0.001$ vs the control.

1
2
3 **Effect of 10d on P-gp in A549/DDP cells.** Previous studies have shown that
4
5 over-expression of P-glycoprotein (P-gp) in cancer cells can export anticancer drugs out
6
7 and cause consequent drug ineffectiveness,^{64,65} which is a leading factor for tumor
8
9 MDR.⁶⁶⁻⁷¹ Thus, to gain more insights into the role of **10d** in suppressing A549/DDP cell
10
11 proliferation, we examined the effect of **10d** on P-gp in A549/DDP cells.
12
13

14
15 We first determined the levels of P-gp expression in A549 and A549/DDP cells using
16
17 Western blot assay. As shown in Figure 8A, high levels of P-gp were expressed in
18
19 A549/DDP cells while only little was detected in A549 cells. Next, the impact of **10d** on
20
21 the levels of P-gp expression was determined by Western blot and reverse
22
23 transcription-PCR (RT-PCR). Treatment with **10d** significantly decreased the relative
24
25 levels of P-gp mRNA transcripts and protein expression in A549/DDP cells (Figure 8B
26
27 and C).
28
29
30

31
32 In addition, the effect of **10d** on P-gp-mediated efflux of rhodamine 123 (Rh123) in
33
34 A549/DDP cells was examined (Figure 8D). Treatment with different concentrations
35
36 (0.03-1.2 μM) of **10d** increased the levels of intracellular Rh123 accumulation in
37
38 A549/DDP cells and the effect of **10d** at 1.2 μM was stronger than that of the positive
39
40 control verapamil (VRP). Collectively, these results suggest that **10d** had potent
41
42 antiproliferative activity against A549/DDP cells by inhibiting P-gp expression in
43
44 drug-resistant human lung cancer cells.
45
46
47
48
49
50
51
52
53
54
55
56
57
58
59
60

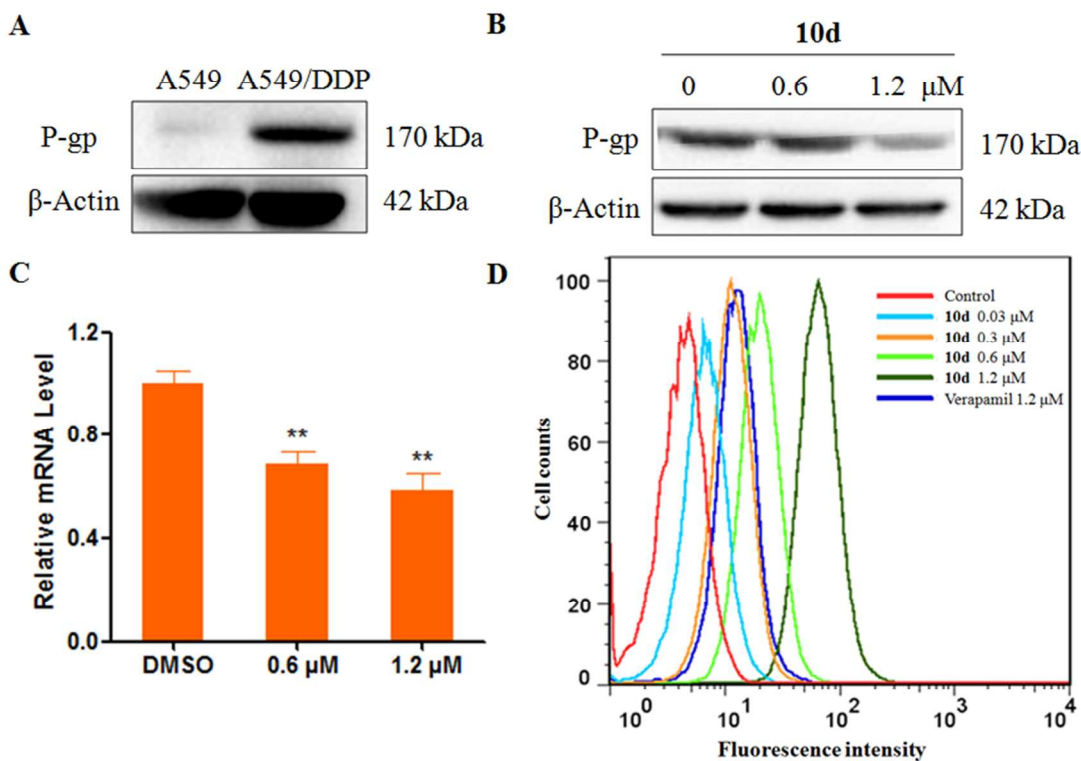


Figure 8. (A) Expression profiles of P-gp in cells. (B) Effect of **10d** on the protein expression of P-gp in A549/DDP cells. Cells were treated with **10d** (0.6 or 1.2 μM) or vehicle for 24 h and the relative levels of P-gp to β -actin expression were determined by Western blot assay. (C) The relative levels of P-gp mRNA transcripts in A549/DDP cells. The cells were treated with compounds for 24 h. The relative levels of P-gp to GAPDH mRNA transcripts were determined by RT-PCR and expressed as fold change of the control (in the presence of 0.1% DMSO). Data are representative of three independent experiments. $**P < 0.01$ vs the DMSO group. (D) The accumulation of rhodamine 123 in A549/DDP cells was analyzed by flow cytometry.

Effect of 10d on P-gp ATPase activity. The efflux of drug by P-gp is dependent on ATP, which is derived from ATP hydrolysis by the ATPase, and the activity of P-gp ATPase is

1
2
3 closely related to the transport capacity of P-gp. To further understand its action, we
4
5 examined the impact of **10d** on the activity of P-gp ATPase in A549/DDP cells using
6
7 Pgp-GloTM assay system (Promega, USA), according to a previously described
8
9 method.^{72,73} We isolated the crude membranes from A549/DDP cells and treated in
10
11 triplicate with **10d** (40 μ M), 200 μ M Sodium vanadate (Na_3VO_4 , a negative control),
12
13 VRP (the inhibitor of P-gp) or vehicle in the presence of MgATP (5 mM, 37 °C, 40 min).
14
15 The RLU (relative light unit) representing the ATP consumed by P-gp ATPase was
16
17 measured using a luminescent detector. The RLU values in the VRP-treated membrane
18
19 samples were significantly lower than that in the vehicle-treated controls (Table 4). In
20
21 contrast, treatment with **10d**, similar to that of negative control Na_3VO_4 , significantly
22
23 increased the values of RLU in A549/DDP cell membranes. Given that the values of
24
25 RLU were negatively correlated with the activities of ATPase in the samples, these data
26
27 indicated that VRP stimulated the ATPase activity while **10d** inhibited the ATPase
28
29 activity.
30
31
32
33
34
35
36
37

38 **Table 4.** Effect of **10d** on P-gp ATPase activity.
39

40	41	42	43
44	45	46	47
Compound	Concentration (μ M)	Luminescence (relative light units) ^a	
Untreated	0	706683 \pm 23554	
VRP	200	641490 \pm 17014*	
Na_3VO_4	200	790447 \pm 12182**	
10d	40	761592 \pm 14162*	

56
57 ^aRelative light units (RLU) represent the levels of ATP in the samples, and are negatively
58
59

1
2
3
4 correlated with activity of P-gp ATPase. Na_3VO_4 , a negative control (not a substrate of
5
6 P-gp); Verapamil, a positive control (a substrate of P-gp). Data are representative of three
7
8 independent experiments. $*P < 0.05$, $**P < 0.01$ vs the untreated group.
9
10

11 12 13 **Antitumor Efficacy of 10d in Inhibiting the Growth of A549/DDP Xenograft Tumors**

14 **in Mice.** To investigate the safety profile of the hybrids, the acute toxicity of **10d** was
15
16 tested in ICR mice at doses of 200, 250, 300, 350, 400, and 450 mg/kg (ip, $n = 10$ per
17
18 group). As shown in Table 5, treatment with **10d** at the lowest dose (200 mg/kg) only
19
20 killed one mouse at day 3 post treatment. However, treatment with **10d** at 450 mg/kg
21
22 killed all the mice. Finally, the median lethal dose (LD_{50}) value of **10d** was calculated to
23
24 be 284.537 mg/kg.
25
26
27

28
29 Next, we tested the in vivo antitumor efficacy of **10d** against A549/DDP xenografts.
30
31 After the solid tumors were established and reached 180-200 mm^3 , the mice were
32
33 randomized and treated intraperitoneally with indicated dose (20 mg/kg or 40 mg/kg) of
34
35 **10d** or the same volume of vehicle consisting of PBS/DMSO/cremophor-EL (8:1:1) daily
36
37 for 15 consecutive days. As shown in Figure 9, treatment with 20 or 40 mg/kg **10d**
38
39 significantly reduced the growth of A549/DDP tumor ($P < 0.01$, $P < 0.001$ vs the control).
40
41 Importantly, the tumor weights (0.49 ± 0.13 g) of mice treated with **10d** at 40 mg/kg were
42
43 significantly reduced by 67 % as compared to the control (1.48 ± 0.11 g, $P < 0.01$, Table
44
45 6). Besides, no mortality or significant weight loss was observed for any of **10d**-treated
46
47 mice during the post-treatment period (Table 6). Together, these results indicated that **10d**
48
49 had potent anticancer activity against the growth of implanted drug-resistant human lung
50
51 cancer cells in mice with little toxicity.
52
53
54
55
56
57
58
59
60

Table 5. Acute toxicity of **10d** in mice.

Dose (mg/kg)	No. of mice	Mouse mortality				Total mortality	Survival (%) on day 14	LD ₅₀ ^a (mg/kg)
		1h	4h	3d	4-14d			
450	10	0	2	8	0	10	0	284.537
400	10	0	0	9	0	9	10	
350	10	0	0	7	0	7	30	
300	10	0	0	5	0	5	50	
250	10	0	0	4	0	4	60	
200	10	0	0	1	0	1	90	

^aThe 95% confidence limits: 248.892-316.481 mg/kg.

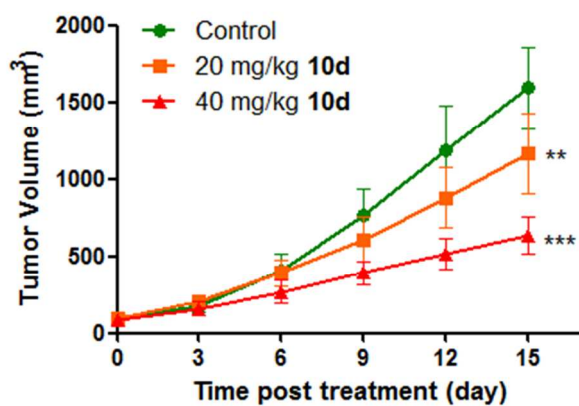


Figure 9. Growth curve of implanted A549/DDP xenografts in nude mice treated with ip of vehicle alone or **10d** (20 or 40 mg/kg). Data are presented as the mean \pm SD ($n = 8$ nude mice per group). ** $P < 0.01$, *** $P < 0.001$ vs the control.

Table 6. Effects of **10d** on the body and tumor weights in mice^a

Group	Dose (mg/kg)	Body weight (g)		Tumor weight (g)	Inhibitory ratio (%, w/w)
		day 1	day 15		
Control	-	19.3 ± 1.55	21.0 ± 1.28	1.48 ± 0.11	-
10d	20	18.3 ± 1.85	18.6 ± 1.75	0.94 ± 0.21 ^b	36
10d	40	19.9 ± 1.64	19.6 ± 1.33	0.49 ± 0.13 ^b	67

^aData are shown as the mean ± SD of body and tumor weights ($n = 8$). ^b $P < 0.01$ vs the control.

CONCLUSIONS

A new series of ligustrazine-curcumin hybrids (**10a-u**) were designed, synthesized and biologically evaluated. We found that compound **10d** displayed strong and selective antiproliferative activity against both drug-sensitive A549, SPC-A-1, LTEP-G-2 and drug-resistant A549/DDP cells. Furthermore, **10d** suppressed TrxR expression and activity, promoted intracellular ROS accumulation and lung cancer cell apoptosis, and its anticancer activity was significantly attenuated by ROS scavengers. Accordingly, the reduced TrxR expression and activity by **10d** in cancer cells may reflect the consequence of apoptosis due to reduced cell viability and energy depletion during apoptosis. Additionally, **10d** inhibited the NF- κ B, AKT and ERK signaling, P-gp-mediated efflux of

1
2
3
4 rhodamine 123, P-gp expression and ATPase activity in A549/DDP cells. Moreover, **10d**
5
6
7 was relatively safe to mice and significantly inhibited the growth of implanted
8
9
10 drug-resistant lung tumor in mice. Together, these results indicate that **10d**, a hybrid of
11
12 ligustrazine and curcumin moiety, has potent anticancer activity preferably against
13
14 drug-resistant lung cancer. Our findings may provide a proof of principle that the hybrids
15
16
17 like **10d** as novel TrxR inhibitors may be promising candidates for the intervention of
18
19
20 drug-sensitive and drug-resistant lung cancer.
21
22
23
24

25 EXPERIMENTAL SECTION

26
27
28 **General Methods.** The reagents commercially available were used without further
29
30 purification, unless noted specifically. The purity of **10a-u** was determined using HPLC
31
32 (see the Supporting Information). Nuclear magnetic resonance (NMR) spectra were
33
34 recorded on a Bruker Avance 300 (¹H, 300 MHz; ¹³C, 75 MHz) or 500 (¹H, 500 MHz;
35
36 ¹³C, 125 MHz) spectrometer at 300 K, using tetramethylsilane (TMS) as an internal
37
38 reference. Melting points (mp) were measured using a Mel-TEMP II apparatus and
39
40 uncorrected. ESI-mass and high-resolution mass spectra (HRMS) were recorded on a
41
42 Water Q-ToF micro mass spectrometer. Infrared (IR) spectra were recorded as KBr
43
44 pellets on a Nicolet Impact 410 instrument. 2-hydroxymethyl-3,5,6- trimethylpyrazine (**7**)
45
46 and intermediates **9a-u** were prepared as described previously.^{52,53} **9a-d** and **9f-u** were
47
48 reported in previous literatures,⁷⁴⁻⁷⁹ while **9e** was an unknown compound and its chemical
49
50
51
52
53
54
55
56
57
58
59
60 characterization is shown in the Supporting Information.

1
2
3 **Synthesis of 3,5,6-trimethylpyrazine-2-carbaldehyde (8)** Compound **7** (1.5 g, 10 mmol)
4 was dissolved in DMSO (15 mL), and cooled to 0 °C. IBX (2.8 g, 11 mmol) was added
5 and the solution was stirred for 0.5 h at room temperature. Then, the reaction mixture was
6 diluted with saturated sodium bicarbonate (NaHCO₃) aqueous solution and extracted with
7 EtOAc. The organic layer was washed with brine, dried with anhydrous sodium sulfate,
8 filtered and evaporated in vacuum. The crude product was purified by column
9 chromatography (PE/EtOAc = 10:1-1:1) to give the title compound **8** as a yellow powder
10 in 100 % yield. mp 90-92 °C; ¹H NMR (300 M Hz, CDCl₃): δ 2.61 (s, 6H, 2 × CH₃), 2.80
11 (s, 3H, CH₃), 10.15 (s, 1H, CHO) ppm; ¹³C NMR (75 M Hz, CDCl₃): δ 20.9, 21.8, 141.4,
12 149.5, 151.0, 154.9, 193.8; MS (ESI): 151 [M+H]⁺.
13
14
15
16
17
18
19
20
21
22
23
24
25
26
27
28

29 **General Procedure for the Preparation of Compounds 10a-u.** BF₃·Et₂O was added
30 (35.6 μL, 0.13 mmol) to the stirred solution of compound **8** (100 mg, 0.26 mmol) and
31 various substituted intermediates **9a-u** (0.28 mmol) in dry 1,4-dioxane at room
32 temperature under a nitrogen atmosphere. The reaction mixture was stirred and refluxed
33 for 4-6 h at 101 °C and cooled to room temperature. And then, the reaction mixture was
34 diluted with saturated NaHCO₃ aqueous solution and extracted with EtOAc. The organic
35 layer was washed with brine, dried with anhydrous sodium sulfate, filtered and
36 evaporated in vacuum. The crude product was purified by column chromatography
37 (PE/EtOAc = 10:1-1:1) to yield the title compounds, respectively.
38
39
40
41
42
43
44
45
46
47
48
49
50
51
52
53

54 **(1E,4E)-1-(2-Hydroxyphenyl)-5-(3,5,6-trimethylpyrazin-2-yl)penta-1,4-dien-3-one**

55
56 **(10a)** Yellow powder; yield 78 %; mp 166-168 °C; IR (KBr, cm⁻¹): 3339, 2914, 1645,
57
58
59
60

1
2
3
4 1612, 1578; ^1H NMR (300 M Hz, DMSO- d_6): δ 2.48 (s, 3H, CH₃), 2.50 (s, 3H, CH₃),
5
6 2.60 (s, 3H, CH₃), 6.85-6.96 (m, 2H, CH=CHCO, Ar-H), 7.28 (t, 1H, J = 7.5, 7.3 Hz,
7
8 Ar-H), 7.38 (d, 1H, J = 16.0 Hz, Ar-H), 7.51 (d, 1H, J = 15.3 Hz, Ar-H), 7.77-7.85 (m,
9
10 2H, CH=CHCO, CH=CHCO), 7.97 (d, 1H, J = 15.0 Hz, CH=CHCO), 10.33 (s, 1H, OH)
11
12 ppm; ^{13}C NMR (75 M Hz, DMSO- d_6): δ 20.4, 21.4, 21.6, 116.2, 119.4, 121.2, 124.6,
13
14 128.4, 129.8, 132.0, 136.3, 138.4, 142.2, 149.3, 149.6, 152.7, 157.2, 188.3; MS (ESI):
15
16 295 [M+H]⁺, 317 [M+Na]⁺; HRMS: calcd for C₁₈H₁₈N₂O₂Na [M+Na]⁺ 317.1266, found
17
18 317.1266.
19
20
21
22
23
24
25
26
27

28 **(1E,4E)-1-(3-Hydroxyphenyl)-5-(3,5,6-trimethylpyrazin-2-yl)penta-1,4-dien-3-one**

29
30 **(10b)** Yellow powder; yield 66 %; mp 220-222 °C; IR (KBr, cm⁻¹): 3339, 3009, 2924,
31
32 1670, 1621, 1592, 1574; ^1H NMR (300 M Hz, DMSO- d_6): δ 2.49 (s, 3H, CH₃), 2.51 (s,
33
34 3H, CH₃), 2.61 (s, 3H, CH₃), 6.87 (d, 1H, J = 15.0 Hz, CH=CHCO), 7.13-7.41 (m, 4H, 4
35
36 × Ar-H), 7.52-7.66 (m, 2H, CH=CHCO, CH=CHCO), 7.85 (d, 1H, J = 15.0 Hz,
37
38 CH=CHCO), 9.66 (s, 1H, OH) ppm; ^{13}C NMR (75 M Hz, DMSO- d_6): δ 20.4, 21.4, 21.6,
39
40 115.1, 117.8, 119.7, 125.3, 129.8, 135.8, 136.8, 142.2, 149.4, 149.6, 152.8, 157.7, 188.3;
41
42 MS (ESI): 295 [M+H]⁺, 317 [M+Na]⁺; HRMS: calcd for C₁₈H₁₈N₂O₂Na [M+Na]⁺
43
44 317.1266, found 317.1266.
45
46
47
48
49
50
51
52
53
54

55 **(1E,4E)-1-(4-Hydroxyphenyl)-5-(3,5,6-trimethylpyrazin-2-yl)penta-1,4-dien-3-one**

56
57 **(10c)** Yellow powder; yield 69 %; mp 249-251 °C; IR (KBr, cm⁻¹): 3220, 3021, 2940,
58
59
60

1
2
3
4 1660, 1617, 1598, 1552; ^1H NMR (300 M Hz, DMSO- d_6): δ 2.48 (s, 3H, CH₃), 2.50 (s,
5
6 3H, CH₃), 2.60 (s, 3H, CH₃), 6.82 (d, 2H, J = 8.5 Hz, 2 \times Ar-H), 7.22 (d, 1H, J = 15.8 Hz,
7
8 CH=CHCO), 7.51 (d, 1H, J = 15.3 Hz, CH=CHCO), 7.63-7.70 (m, 3H, CH=CHCO, 2 \times
9
10 Ar-H), 7.80 (d, 1H, J = 15.3 Hz, CH=CHCO), 10.12 (s, 1H, OH) ppm; ^{13}C NMR (75 M
11
12 Hz, DMSO- d_6): δ 20.4, 21.4, 21.6, 115.8, 122.3, 125.6, 130.0, 130.9, 136.1, 142.3, 143.5,
13
14 149.3, 149.6, 152.6, 160.2, 187.9; MS (ESI): 295 [M+H]⁺, 317 [M+Na]⁺; HRMS: calcd
15
16 for C₁₈H₁₈N₂O₂Na [M+Na]⁺ 317.1266, found 317.1268.
17
18
19
20
21
22
23
24

25
26 **(1E,4E)-1-(4-Hydroxy-3-methoxyphenyl)-5-(3,5,6-trimethylpyrazin-2-yl)penta-1,4-di**
27
28 **en-3-one (10d)** Yellow powder; yield 63 %; mp 194-196 °C; IR (KBr, cm⁻¹): 3398, 3062,
29
30 2921, 1671, 1646, 1621, 1574; ^1H NMR (300 M Hz, CDCl₃): δ 2.55 (s, 3H, CH₃), 2.56 (s,
31
32 3H, CH₃), 2.65 (s, 3H, CH₃), 3.94 (s, 3H, OCH₃), 6.31 (s, 1H, OH), 6.88-6.96 (m, 2H,
33
34 CH=CHCO, Ar-H), 7.13-7.19 (m, 2H, 2 \times Ar-H), 7.71-7.78 (m, 2H, CH=CHCO,
35
36 CH=CHCO), 7.88 (d, 1H, J = 15.0 Hz, CH=CHCO) ppm; ^{13}C NMR (75 M Hz, CDCl₃): δ
37
38 20.8, 21.8, 22.0, 56.0, 109.7, 115.0, 123.8, 124.5, 127.3, 129.0, 136.5, 143.2, 144.2, 147.0,
39
40 148.5, 149.7, 149.8, 152.6, 188.8; MS (ESI): 325 [M+H]⁺, 347 [M+Na]⁺; HRMS: calcd
41
42 for C₁₉H₂₀N₂O₃Na [M+Na]⁺ 347.1372, found 347.1383.
43
44
45
46
47
48
49
50
51

52
53 **(1E,4E)-1-(2-Hydroxy-3-methoxyphenyl)-5-(3,5,6-trimethylpyrazin-2-yl)penta-1,4-di**
54
55 **en-3-one (10e)** Yellow powder; yield 67 %; mp 177-179 °C; IR (KBr, cm⁻¹): 3367, 3056,
56
57 2922, 1658, 1618, 1574; ^1H NMR (300 M Hz, CDCl₃): δ 2.54 (s, 3H, CH₃), 2.56 (s, 3H,
58
59

1
2
3
4 CH₃), 2.65 (s, 3H, CH₃), 3.92 (s, 3H, OCH₃), 6.37 (s, 1H, OH), 6.87-6.89 (m, 2H,
5
6 CH=CHCO, Ar-H), 7.17-7.27 (m, 2H, 2 × Ar-H), 7.75 (d, 1H, *J* = 15.1 Hz, CH=CHCO),
7
8
9 7.88 (d, 1H, *J* = 15.1 Hz, CH=CHCO), 8.04 (d, 1H, *J* = 16.2 Hz, CH=CHCO) ppm; ¹³C
10
11 NMR (75 M Hz, CDCl₃): δ 20.8, 21.8, 22.0, 56.2, 112.0, 119.8, 121.1, 127.7, 129.3,
12
13 136.6, 138.8, 143.3, 145.8, 146.9, 149.6, 152.5, 189.6; MS (ESI): 325 [M+H]⁺; HRMS:
14
15 calcd for C₁₉H₂₀N₂O₃Na [M+Na]⁺ 347.1372, found 347.1381.
16
17
18
19
20
21
22

23 **(1*E*,4*E*)-1-(2-Methoxyphenyl)-5-(3,5,6-trimethylpyrazin-2-yl)penta-1,4-dien-3-one**

24
25 **(10f)** Yellow powder; yield 57 %; mp 134-136 °C; IR (KBr, cm⁻¹): 3067, 2914, 1645,
26
27 1591, 1572; ¹H NMR (300 M Hz, CDCl₃): δ 2.53 (s, 3H, CH₃), 2.56 (s, 3H, CH₃), 2.65 (s,
28
29 3H, CH₃), 3.92 (s, 3H, OCH₃), 6.92-7.01 (m, 2H, CH=CHCO, Ar-H), 7.11 (d, 1H, *J* =
30
31 16.2 Hz, Ar-H), 7.38 (t, 1H, *J* = 7.3 Hz, Ar-H), 7.59 (d, 1H, *J* = 6.9 Hz, Ar-H), 7.73 (d,
32
33 1H, *J* = 15.1 Hz, CH=CHCO), 7.87 (d, 1H, *J* = 15.1 Hz, CH=CHCO), 8.09 (d, 1H, *J* =
34
35 16.2 Hz, CH=CHCO) ppm; ¹³C NMR (75 M Hz, CDCl₃): δ 20.3, 21.3, 21.5, 55.0, 110.7,
36
37 120.3, 123.2, 126.7, 128.5, 128.8, 131.4, 136.1, 138.8, 142.7, 149.1, 149.3, 152.0, 158.2,
38
39 189.0; MS (ESI): 331 [M+Na]⁺; HRMS: calcd for C₁₉H₂₀N₂O₂Na [M+Na]⁺ 331.1422,
40
41
42
43
44
45
46
47 found 331.1429.
48
49
50
51

52 **(1*E*,4*E*)-1-(3-Methoxyphenyl)-5-(3,5,6-trimethylpyrazin-2-yl)penta-1,4-dien-3-one**

53
54
55 **(10g)** Yellow powder; yield 73 %; mp 128-130 °C; IR (KBr, cm⁻¹): 3050, 2918, 1670,
56
57 1620, 1575; ¹H NMR (300 M Hz, CDCl₃): δ 2.54 (s, 3H, CH₃), 2.56 (s, 3H, CH₃), 2.65 (s,
58
59

1
2
3
4 3H, CH₃), 3.85 (s, 3H, OCH₃), 6.95-7.06 (m, 2H, CH=CHCO, Ar-H), 7.13 (s, 1H, Ar-H),
5
6 7.20-7.36 (m, 2H, 2 × Ar-H), 7.72 (d, 2H, *J* = 14.9 Hz, CH=CHCO, CH=CHCO), 7.88 (d,
7
8 1H, *J* = 15.0 Hz, CH=CHCO) ppm; ¹³C NMR (75 M Hz, CDCl₃): δ 20.3, 21.3, 21.6, 54.8,
9
10 112.7, 116.0, 120.7, 126.3, 128.3, 129.5, 135.6, 136.5, 142.5, 143.2, 149.2, 149.4, 152.2,
11
12 159.5, 188.4; MS (ESI): 309 [M+H]⁺, 331 [M+Na]⁺; HRMS: calcd for C₁₉H₂₀N₂O₂Na
13
14 [M+Na]⁺ 331.1422, found 331.1415.
15
16
17
18
19
20
21
22

23 **(1E,4E)-1-(4-Methoxyphenyl)-5-(3,5,6-trimethylpyrazin-2-yl)penta-1,4-dien-3-one**

24
25 **(10h)** Yellow powder; yield 67 %; mp 118-120 °C; IR (KBr, cm⁻¹): 2920, 1664, 1621,
26
27 1604, 1584; ¹H NMR (300 M Hz, CDCl₃): δ 2.54 (s, 3H, CH₃), 2.56 (s, 3H, CH₃), 2.65 (s,
28
29 3H, CH₃), 3.86 (s, 3H, OCH₃), 6.91-6.96 (m, 3H, CH=CHCO, 2 × Ar-H), 7.57 (d, 2H, *J* =
30
31 8.7 Hz, 2 × Ar-H), 7.71-7.79 (m, 2H, CH=CHCO, CH=CHCO), 7.87 (d, 1H, *J* = 15.0 Hz,
32
33 CH=CHCO) ppm; ¹³C NMR (75 M Hz, CDCl₃): δ 20.4, 21.3, 21.6, 54.9, 114.0, 123.9,
34
35 127.0, 128.7, 129.7, 136.0, 142.7, 143.2, 149.1, 149.3, 152.1, 161.3, 188.4; MS (ESI):
36
37 309 [M+H]⁺, 331 [M+Na]⁺; HRMS: calcd for C₁₉H₂₀N₂O₂Na [M+Na]⁺ 331.1422, found
38
39 331.1413.
40
41
42
43
44
45
46
47
48
49

50 **(1E,4E)-1-(3,4-Dimethoxyphenyl)-5-(3,5,6-trimethylpyrazin-2-yl)penta-1,4-dien-3-on**

51
52 **e (10i)** Yellow powder; yield 49 %; mp 116-118 °C; IR (KBr, cm⁻¹): 3013, 2920, 1661,
53
54 1615, 1570; ¹H NMR (300 M Hz, CDCl₃): δ 2.54 (s, 3H, CH₃), 2.56 (s, 3H, CH₃), 2.65 (s,
55
56 3H, CH₃), 3.94 (s, 3H, OCH₃), 3.95 (s, 3H, OCH₃), 6.89-6.96 (m, 2H, CH=CHCO, Ar-H),
57
58
59
60

1
2
3
4 7.15-7.30 (m, 2H, 2 × Ar-H), 7.72-7.78 (m, 2H, CH=CHCO, CH=CHCO), 7.88 (d, 1H, J
5 = 15.0 Hz, CH=CHCO) ppm; ^{13}C NMR (75 M Hz, CDCl_3): δ 20.3, 21.3, 21.5, 55.4, 55.5,
6
7
8 109.3, 110.6, 122.9, 124.3, 127.2, 128.4, 136.1, 142.6, 143.4, 148.8, 149.2, 149.3, 151.0,
9
10
11 152.1, 188.2; MS (ESI): 339 $[\text{M}+\text{H}]^+$, 361 $[\text{M}+\text{Na}]^+$; HRMS: calcd for $\text{C}_{20}\text{H}_{22}\text{N}_2\text{O}_3\text{Na}$
12
13 $[\text{M}+\text{Na}]^+$ 361.1528, found 361.1536.
14
15
16
17
18
19

20 **(1E,4E)-1-(2,4-Dimethoxyphenyl)-5-(3,5,6-trimethylpyrazin-2-yl)penta-1,4-dien-3-on**
21
22 **e (10j)** Yellow powder; yield 54 %; mp 121-123 °C; IR (KBr, cm^{-1}): 3014, 2920, 1661,
23
24 1612, 1567; ^1H NMR (300 M Hz, CDCl_3): δ 2.54 (s, 3H, CH_3), 2.56 (s, 3H, CH_3), 2.65 (s,
25
26 3H, CH_3), 3.86 (s, 3H, OCH_3), 3.91 (s, 3H, OCH_3), 6.46-6.55 (m, 2H, 2 × Ar-H), 7.03 (d,
27
28 1H, J = 16.1 Hz, CH=CHCO), 7.54 (d, 1H, J = 8.6 Hz, Ar-H), 7.71 (d, 1H, J = 15.1 Hz,
29
30 CH=CHCO), 7.86 (d, 1H, J = 15.1 Hz, CH=CHCO), 8.03 (d, 1H, J = 16.1 Hz,
31
32 CH=CHCO) ppm; ^{13}C NMR (75 M Hz, CDCl_3): δ 20.8, 21.8, 22.0, 55.5, 98.4, 105.5,
33
34 116.8, 124.9, 129.6, 130.6, 136.1, 139.4, 143.3, 149.5, 149.7, 152.3, 160.3, 163.2, 189.4;
35
36 MS (ESI): 339 $[\text{M}+\text{H}]^+$, 361 $[\text{M}+\text{Na}]^+$; HRMS: calcd for $\text{C}_{20}\text{H}_{22}\text{N}_2\text{O}_3\text{Na}$ $[\text{M}+\text{Na}]^+$
37
38 361.1528, found 361.1541.
39
40
41
42
43
44
45
46
47
48
49

50 **(1E,4E)-1-(3,4,5-Trimethoxyphenyl)-5-(3,5,6-trimethylpyrazin-2-yl)penta-1,4-dien-3-**
51
52 **one (10k)** Yellow powder; yield 68 %; mp 131-133 °C; IR (KBr, cm^{-1}): 3068, 2914, 1650,
53
54 1619, 1578; ^1H NMR (300 M Hz, CDCl_3): δ 2.55 (s, 3H, CH_3), 2.57 (s, 3H, CH_3), 2.66 (s,
55
56 3H, CH_3), 3.93 (s, 9H, 3 × OCH_3), 6.86 (s, 2H, 2 × Ar-H), 6.93 (d, 1H, J = 15.0 Hz,
57
58
59
60

1
2
3
4 CH=CHCO), 7.69-7.79 (m, 2H, CH=CHCO, CH=CHCO), 7.90 (d, 1H, $J = 15.0$ Hz,
5
6 CH=CHCO) ppm; ^{13}C NMR (75 M Hz, CDCl_3): δ 20.3, 21.3, 21.6, 55.7, 60.5, 105.2,
7
8
9 125.6, 128.2, 129.7, 130.4, 136.4, 140.0, 142.5, 143.4, 149.2, 149.3, 152.2, 153.0, 188.2;
10
11 MS (ESI): 369 $[\text{M}+\text{H}]^+$, 391 $[\text{M}+\text{Na}]^+$; HRMS: calcd for $\text{C}_{21}\text{H}_{24}\text{N}_2\text{O}_4\text{Na}$ $[\text{M}+\text{Na}]^+$
12
13 391.1634, found 391.1635.
14
15
16
17
18
19

20 **(1E,4E)-1-(Benzo[d][1,3]dioxol-5-yl)-5-(3,5,6-trimethylpyrazin-2-yl)penta-1,4-dien-3**
21
22 **-one (10l)** Yellow powder; yield 77 %; mp 148-150 °C; IR (KBr, cm^{-1}): 3015, 2914, 1661,
23
24 1619, 1577; ^1H NMR (300 M Hz, CDCl_3): δ 2.54 (s, 3H, CH_3), 2.56 (s, 3H, CH_3), 2.65 (s,
25
26 3H, CH_3), 6.03 (s, 2H, OCH_2O), 6.83-6.91 (m, 2H, CH=CHCO, Ar-H), 7.10 (d, 2H, $J =$
27
28 8.4 Hz, $2 \times$ Ar-H), 7.68-7.74 (m, 2H, CH=CHCO, CH=CHCO), 7.86 (d, 1H, $J = 15.0$ Hz,
29
30 CH=CHCO) ppm; ^{13}C NMR (75 M Hz, CDCl_3): δ 20.3, 21.3, 21.6, 101.1, 106.1, 108.2,
31
32 124.2, 124.7, 128.7, 136.2, 142.6, 143.2, 147.9, 149.2, 149.3, 149.5, 152.1, 188.2; MS
33
34 (ESI): 323 $[\text{M}+\text{H}]^+$, 345 $[\text{M}+\text{Na}]^+$; HRMS: calcd for $\text{C}_{19}\text{H}_{18}\text{N}_2\text{O}_3\text{Na}$ $[\text{M}+\text{Na}]^+$ 345.1215,
35
36 found 345.1207.
37
38
39
40
41
42
43
44
45
46

47 **(1E,4E)-1-Phenyl-5-(3,5,6-trimethylpyrazin-2-yl)penta-1,4-dien-3-one (10m)** Yellow
48
49 powder; yield 74 %; mp 115-117 °C; IR (KBr, cm^{-1}): 3064, 2918, 1672, 1622, 1591; ^1H
50
51 NMR (300 M Hz, CDCl_3): δ 2.53 (s, 3H, CH_3), 2.55 (s, 3H, CH_3), 2.66 (s, 3H, CH_3), 7.01
52
53 (d, 1H, $J = 15.0$ Hz, CH=CHCO), 7.40-7.42 (m, 3H, $3 \times$ Ar-H), 7.60-7.61 (m, 2H, $2 \times$
54
55 Ar-H), 7.72-7.80 (m, 2H, CH=CHCO, CH=CHCO), 7.88 (d, 1H, $J = 15.0$ Hz,
56
57
58
59
60

1
2
3
4 $\underline{\text{CH}}=\text{CHCO}$) ppm; ^{13}C NMR (75 M Hz, CDCl_3): δ 20.4, 21.3, 21.6, 126.0, 128.0, 128.4,
5
6
7 128.5, 130.1, 134.2, 136.5, 142.5, 143.3, 149.2, 149.4, 152.4, 188.4; MS (ESI): 279
8
9 $[\text{M}+\text{H}]^+$, 301 $[\text{M}+\text{Na}]^+$; HRMS: calcd for $\text{C}_{18}\text{H}_{18}\text{N}_2\text{ONa}$ $[\text{M}+\text{Na}]^+$ 301.1317, found
10
11 301.1308.
12
13

14
15
16
17
18 **(1E,4E)-1-(4-Fluorophenyl)-5-(3,5,6-trimethylpyrazin-2-yl)penta-1,4-dien-3-one (10n)**

19
20 Yellow powder; yield 60 %; mp 114-116 °C; IR (KBr, cm^{-1}): 3044, 2914, 1670, 1625,
21
22 1586; ^1H NMR (300 M Hz, CDCl_3): δ 2.55 (s, 3H, CH_3), 2.56 (s, 3H, CH_3), 2.66 (s, 3H,
23
24 CH_3), 6.95 (d, 1H, $J = 15.0$ Hz, $\text{CH}=\underline{\text{CH}}\text{CO}$), 7.09-7.14 (m, 2H, $2 \times \text{Ar-H}$), 7.59-7.64 (m,
25
26 CH_3), 6.95 (d, 1H, $J = 15.0$ Hz, $\text{CH}=\underline{\text{CH}}\text{CO}$), 7.09-7.14 (m, 2H, $2 \times \text{Ar-H}$), 7.59-7.64 (m,
27
28 2H, $2 \times \text{Ar-H}$), 7.71-7.77 (m, 2H, $\text{CH}=\underline{\text{CH}}\text{CO}$, $\underline{\text{CH}}=\text{CHCO}$), 7.89 (d, 1H, $J = 15.0$ Hz,
29
30 $\underline{\text{CH}}=\text{CHCO}$) ppm; ^{13}C NMR (75 M Hz, CDCl_3): δ 20.8, 21.8, 22.1, 116.0, 116.3, 126.3,
31
32 128.9, 130.3, 130.4, 131.0, 137.1, 142.5, 143.0, 149.8, 152.8, 165.8, 188.7; MS (ESI):
33
34 297 $[\text{M}+\text{H}]^+$, 319 $[\text{M}+\text{Na}]^+$; HRMS: calcd for $\text{C}_{18}\text{H}_{17}\text{FN}_2\text{ONa}$ $[\text{M}+\text{Na}]^+$ 319.1223, found
35
36 319.1232.
37
38
39
40
41
42
43

44 **(1E,4E)-1-(4-Chlorophenyl)-5-(3,5,6-trimethylpyrazin-2-yl)penta-1,4-dien-3-one**

45
46
47 **(10o)** Yellow powder; yield 70 %; mp 109-111 °C; IR (KBr, cm^{-1}): 3021, 2926, 1670,
48
49 1624, 1590; ^1H NMR (300 M Hz, CDCl_3): δ 2.55 (s, 3H, CH_3), 2.56 (s, 3H, CH_3), 2.66 (s,
50
51 3H, CH_3), 6.99 (d, 1H, $J = 15.0$ Hz, $\text{CH}=\underline{\text{CH}}\text{CO}$), 7.38 (d, 2H, $J = 8.5$ Hz, $2 \times \text{Ar-H}$), 7.54
52
53 (d, 2H, $J = 8.5$ Hz, $2 \times \text{Ar-H}$), 7.70 (d, 2H, $J = 15.0$ Hz, $\text{CH}=\underline{\text{CH}}\text{CO}$, $\underline{\text{CH}}=\text{CHCO}$), 7.89
54
55 (d, 1H, $J = 15.0$ Hz, $\underline{\text{CH}}=\text{CHCO}$) ppm; ^{13}C NMR (75 M Hz, CDCl_3): δ 20.3, 21.3, 21.6,
56
57
58
59
60

1
2
3
4 126.4, 128.3, 128.8, 129.1, 132.7, 136.0, 136.7, 141.8, 142.4, 149.3, 149.4, 152.3, 188.2;

5
6 MS (ESI): 313 [M+H]⁺, 335 [M+Na]⁺; HRMS: calcd for C₁₈H₁₇ClN₂ONa [M+Na]⁺
7
8 335.0927, found 335.0932.
9
10

11
12
13
14 **(1E,4E)-1-(4-(Trifluoromethyl)phenyl)-5-(3,5,6-trimethylpyrazin-2-yl)penta-1,4-dien**
15
16 **-3-one (10p)** Yellow powder; yield 53 %; mp 117-119 °C; IR (KBr, cm⁻¹): 3062, 2920,
17
18 1672, 1620, 1591; ¹H NMR (300 M Hz, CDCl₃): δ 2.55 (s, 3H, CH₃), 2.57 (s, 3H, CH₃),
19
20 2.66 (s, 3H, CH₃), 7.08 (d, 1H, *J* = 16.1 Hz, CH=CHCO), 7.66-7.81 (m, 6H, 4 × Ar-H,
21
22 CH=CHCO, CH=CHCO), 7.91 (d, 1H, *J* = 15.1 Hz, CH=CHCO) ppm; ¹³C NMR (125 M
23
24 Hz, CDCl₃): δ 20.8, 21.7, 22.0, 123.8 (q, *J* = 270 Hz, CF₃), 125.9, 128.4, 128.5, 128.7,
25
26 132.1 (q, *J* = 32 Hz), 137.6, 138.2, 141.6, 142.8, 149.9, 152.9, 188.5; MS (ESI): 347
27
28 [M+H]⁺, 369 [M+Na]⁺; HRMS: calcd for C₁₉H₁₇F₃N₂ONa [M+Na]⁺ 369.1191, found
29
30 369.1188.
31
32
33
34
35
36
37
38
39
40

41
42 **(1E,4E)-1-(*p*-Tolyl)-5-(3,5,6-trimethylpyrazin-2-yl)penta-1,4-dien-3-one (10q)** Yellow
43
44 powder; yield 65 %; mp 118-120 °C; IR (KBr, cm⁻¹): 3050, 2917, 1667, 1619, 1587; ¹H
45
46 NMR (300 M Hz, CDCl₃): δ 2.39 (s, 3H, CH₃), 2.54 (s, 3H, CH₃), 2.56 (s, 3H, CH₃), 2.66
47
48 (s, 3H, CH₃), 6.99 (d, 1H, *J* = 15.0 Hz, CH=CHCO), 7.24 (d, 2H, *J* = 8.0 Hz, 2 × Ar-H),
49
50 7.51 (d, 2H, *J* = 8.1 Hz, 2 × Ar-H), 7.72-7.80 (m, 2H, CH=CHCO, CH=CHCO), 7.88 (d,
51
52 1H, *J* = 15.0 Hz, CH=CHCO) ppm; ¹³C NMR (75 M Hz, CDCl₃): δ 20.8, 21.5, 21.8, 22.0,
53
54 125.7, 128.5, 129.1, 129.7, 132.0, 136.7, 141.2, 143.1, 143.9, 149.6, 149.9, 152.6, 189.0;
55
56
57
58
59
60

MS (ESI): 293 [M+H]⁺, 315 [M+Na]⁺; HRMS: calcd for C₁₉H₂₀N₂ONa [M+Na]⁺
315.1473, found 315.1481.

(1E,4E)-1-(2-Nitrophenyl)-5-(3,5,6-trimethylpyrazin-2-yl)penta-1,4-dien-3-one (10r)

Yellow powder; yield 58 %; mp 116-118 °C; IR (KBr, cm⁻¹): 3038, 2914, 1671, 1622,
1592, 1522, 1348; ¹H NMR (300 M Hz, CDCl₃): δ 2.55 (s, 3H, CH₃), 2.56 (s, 3H, CH₃),
2.66 (s, 3H, CH₃), 6.88 (d, 1H, *J* = 16.0 Hz, CH=CHCO), 7.58 (t, 1H, *J* = 8.3 Hz, Ar-H),
7.67-7.78 (m, 3H, CH=CHCO, 2 × Ar-H), 7.91 (d, 1H, *J* = 15.1 Hz, CH=CHCO), 8.07 (d,
1H, *J* = 8.0 Hz, Ar-H), 8.15 (d, 1H, *J* = 16.0 Hz, CH=CHCO) ppm; ¹³C NMR (75 M Hz,
CDCl₃): δ 20.8, 21.7, 22.1, 125.0, 128.1, 129.2, 130.4, 131.1, 131.2, 133.5, 138.1, 138.8,
142.8, 149.8, 150.0, 153.0, 188.8; MS (ESI): 324 [M+H]⁺; HRMS: calcd for
C₁₈H₁₇N₃O₃Na [M+Na]⁺ 346.1168, found 346.1161.

(1E,4E)-1-(3-Nitrophenyl)-5-(3,5,6-trimethylpyrazin-2-yl)penta-1,4-dien-3-one (10s)

Yellow powder; yield 77 %; mp 185-187 °C; IR (KBr, cm⁻¹): 3063, 2919, 1671, 1625,
1591, 1532, 1350; ¹H NMR (300 M Hz, CDCl₃): δ 2.56 (s, 3H, CH₃), 2.57 (s, 3H, CH₃),
2.67 (s, 3H, CH₃), 7.14 (d, 1H, *J* = 16.1 Hz, CH=CHCO), 7.63 (t, 1H, *J* = 8.0 Hz, Ar-H),
7.73-7.83 (m, 2H, CH=CHCO, CH=CHCO), 7.91-7.97 (m, 2H, CH=CHCO, Ar-OH),
8.25 (d, 1H, *J* = 7.7 Hz, Ar-H), 8.49 (s, 1H, Ar-OH) ppm; ¹³C NMR (75 M Hz, CDCl₃): δ
20.8, 21.8, 22.1, 122.6, 124.7, 128.6, 128.8, 130.0, 134.0, 136.5, 137.9, 140.6, 142.7,
148.7, 149.9, 150.0, 153.1, 188.2; MS (ESI): 324 [M+H]⁺, 346 [M+Na]⁺; HRMS: calcd

1
2
3
4 for $C_{18}H_{17}N_3O_3Na$ $[M+Na]^+$ 346.1168, found 346.1176.
5
6
7
8

9
10 **(1E,4E)-1-(4-Nitrophenyl)-5-(3,5,6-trimethylpyrazin-2-yl)penta-1,4-dien-3-one (10t)**

11
12 Yellow powder; yield 64 %; mp 191-193 °C; IR (KBr, cm^{-1}): 3013, 2919, 1670, 1621,
13
14 1603, 1512, 1343; 1H NMR (300 M Hz, $CDCl_3$): δ 2.56 (s, 3H, CH_3), 2.57 (s, 3H, CH_3),
15
16 2.67 (s, 3H, CH_3), 7.13 (d, 1H, $J = 16.1$ Hz, $CH=CHCO$), 7.72-7.82 (m, 4H, $CH=CHCO$,
17
18 $CH=CHCO$, $2 \times ArOH$), 7.92 (d, 1H, $J = 15.0$ Hz, $CH=CHCO$), 8.27 (d, 2H, $J = 7.7$ Hz,
19
20 $2 \times Ar-H$) ppm; ^{13}C NMR (75 M Hz, $CDCl_3$): δ 20.8, 21.8, 22.1, 124.2, 128.5, 128.9,
21
22 129.9, 130.3, 131.5, 138.0, 140.4, 140.9, 142.7, 148.6, 149.9, 150.0, 153.2, 188.2; MS
23
24 (ESI): 324 $[M+H]^+$; HRMS: calcd for $C_{18}H_{18}N_3O_3$ $[M+H]^+$ 324.1348, found 324.1359.
25
26
27
28
29
30
31
32

33
34 **(1E,4E)-1-(Naphthalen-2-yl)-5-(3,5,6-trimethylpyrazin-2-yl)penta-1,4-dien-3-one**

35
36 **(10u)** Yellow powder; yield 55 %; mp 151-153 °C; IR (KBr, cm^{-1}): 3056, 2914, 1664,
37
38 1622, 1585; 1H NMR (300 M Hz, $CDCl_3$): δ 2.55 (s, 3H, CH_3), 2.58 (s, 3H, CH_3), 2.67 (s,
39
40 3H, CH_3), 7.14 (d, 1H, $J = 16.0$ Hz, $CH=CHCO$), 7.50-7.57 (m, 2H, $2 \times ArOH$),
41
42 7.75-8.04 (m, 7H, $CH=CHCO$, $2 \times CH=CHCO$, $4 \times Ar-OH$) ppm; ^{13}C NMR (75 M Hz,
43
44 $CDCl_3$): δ 20.9, 21.8, 22.1, 123.6, 126.7, 126.8, 127.4, 127.8, 128.7, 128.8, 129.0, 130.7,
45
46 132.3, 133.4, 134.4, 137.0, 143.1, 143.9, 149.7, 149.9, 152.7, 188.9; MS (ESI): 329
47
48 $[M+H]^+$, 351 $[M+Na]^+$; HRMS: calcd for $C_{22}H_{20}N_2ONa$ $[M+Na]^+$ 351.1473, found
49
50 351.1462.
51
52
53
54
55
56
57
58
59
60

1
2
3
4 **MTT Assay.** A549, A549/DDP, SPC-A-1, LTEP-G-2 and HBE cells were seeded in
5
6
7 96-well plates, then treated with vehicle alone or tested compounds for 72 h. 20 μ L of
8
9
10 MTT (5 mg/mL, in PBS) was added to each well and further incubated for another 4 h.
11
12 The MTT formazan formed by viable cells was dissolved in DMSO (150 μ L), and
13
14
15 absorbance was measured using a microplate reader (570 nm).
16

17
18
19 **Apoptosis Analysis.** Cells were incubated in six-well plates (1×10^5 /well) and treated
20
21 with DMSO (1%), **10d**, ligustrazine or curcumin for 24h. The cells were collected,
22
23
24 washed with PBS, and stained with FITC-Annexin-V and PI. Apoptosis was determined
25
26
27 by flow cytometry.
28

29
30
31
32 **Western Blotting.** Cells were incubated in six-well plates (1×10^6 /well) overnight and
33
34
35 treated with vehicle DMSO (0.1%, v/v) alone or **10d** for 24 h. The cells were harvested
36
37
38 and lysed at 4 $^{\circ}$ C for 30 min in a lysis buffer [50 mM Tris, pH 7.4, 1 mM $MgCl_2$, 100 mM
39
40 $NaCl_2$, 2.5 mM EDTA, 0.5% Triton X-100, 1 mM phenylmethanesulfonyl fluoride
41
42 (PMSF), 2.5 mM Na_3VO_4 , 0.5% NP-40, pepstatin A, leupeptin, and 5 g/mL of aprotinin].
43
44
45 The cell lysates were centrifuged at 15,000 rpm for 15 min at 4 $^{\circ}$ C and the supernatants
46
47
48 were collected. The protein concentration in the cell lysates was determined using the
49
50
51 bicinchoninic acid protein assay kit. Protein samples were separated by
52
53
54 SDS-polyacrylamide gel electrophoresis (7.5% gel, 20 μ g per lane) and then transferred
55
56
57 to polyvinylidene difluoride (PVDF) membranes. The membranes were blocked with
58
59
60

1
2
3
4 skim milk (5%) in Tris-buffered saline containing 0.05% Tween 20 and sequentially
5
6 incubated with primary antibodies [anti-Akt, anti-Bcl-2, anti-Bax, anti-Caspase3,
7
8 anti-cleaved Caspase3, anti-ERK, anti-PARP, anti-cleaved PARP, anti-phospho-Akt
9
10 (Ser473), anti-P-gp, anti-GAPDH, anti- β -actin, anti-TrxR, anti-Trx, and
11
12 anti-phospho-ERK (Thr202/Tyr204) antibodies (Cell Signaling, Boston, MA)] and
13
14 followed by enhanced chemiluminescence detection.
15
16
17
18
19
20
21
22

23 **Measurement of ROS generation.** Cells were incubated with vehicle DMSO (0.1%, v/v)
24
25 alone, **10d**, ligustrazine **1** or curcumin **2** for 60 min and the cells were stained with
26
27 dihydroethidium (DHE, Beyotime).^{56,80} The levels of intracellular ROS were examined
28
29 for measuring the fluorescent signals using a fluorescence microplate reader (300 and 610
30
31 nm).
32
33
34
35
36
37
38

39 **Determination of TrxR activity in Cell-free assay.** The NADPH-reduced TrxR (0.16
40
41 μ M) was incubated in triplicate with vehicle DMSO (0.1%, v/v) alone or different
42
43 concentrations of **10d**, **10e**, **10i-k**, ligustrazine **1**, and curcumin **2** in 50 μ L of reaction
44
45 buffer in 96-well plates for 2 h. The mixtures were reacted with 2 mM DTNB and 200
46
47 μ M NADPH for 3 min and the absorbance was determined by a microplate
48
49 spectrophotometer (412 nm). IC₅₀ values of individual compounds were calculated.
50
51
52
53
54
55
56
57

58 **Determination of TrxR activity in Cells.** The impact of **10d** on the TrxR activity in
59
60

1
2
3
4 A549 and A549/DDP cells was determined using a Thioredoxin Reductase Assay Kit
5
6 (Cayman).³⁷ Briefly, cells were incubated with tested compounds (**10d**, **10e**, **10i-k**, **1** and
7
8 **2**) for 24 h. The cells were harvested and homogenized, followed by centrifugation. After
9
10 quantification of protein concentrations, the cell protein samples (50 µg per sample) were
11
12 reacted in triplicate with NADPH (40 mg/ml) and DTNB (10 mM) in TE buffer in
13
14 96-well plates at 37 °C for 1 h. The contents of free TNB derived from free thiols were
15
16 determined by a microplate spectrophotometer (412 nm). The TrxR activity was
17
18 calculated based on the standard curve established using the purified TrxR provided.
19
20
21
22
23
24
25
26

27 **P-gp ATPase assay.** P-gp ATPase assay was carried out according to the manufacturers'
28
29 instruction (P-gp-GloTM Assay System without P-glycoprotein, Promega, USA) with
30
31 minor modification. Briefly, crude membrane samples in 10 mM Tris-HCl (pH 7.5) were
32
33 prepared from A549/DDP cells and individual membrane samples (0.6 mg/mL) were
34
35 treated in triplicate with **10d** (40 µM), 200 µM sodium vanadate (Na₃VO₄, inhibitor) and
36
37 VRP (substrate control) or vehicle in the presence of MgATP (5 mM, 37 °C, 40 min). The
38
39 relative light units (RLU) in individual samples were determined using a luminescent
40
41 detector (Beckman Coulter, USA). The changes in the values of RLU represent the ATP
42
43 consumed by the membrane ATPase and the values of RLU were negatively correlated
44
45 with the activities of ATPase in the samples.
46
47
48
49
50
51
52
53

54 **Real Time Reverse Transcription PCR (RT-PCR).** A549/DDP cells (1 × 10⁶) were
55
56 treated with vehicle control or **10d** (0.6 or 1.2 µM) for 24 h. Total RNA was extracted
57
58
59
60

1
2
3
4 from individual groups of cells using RNASimple Total RNA Kit (TIANGEN BIOTECH,
5
6 DP419) and reversely transcribed into cDNA using oligo dT primers and RevertAid First
7
8 Strand cDNA synthesis kit (Fermentas, Lot: 00104039) following the manufacturer's
9
10 instruction. The relative levels of ABCB1 mRNA transcripts to the control GAPDH in
11
12 individual groups of cells were analyzed by RT-PCR using specific primers, as previously
13
14 described.⁸¹⁻⁸²
15
16
17
18
19
20
21
22
23

24 **In Vivo Experiments.** The in vivo experiments were performed at the Cancer Research
25
26 Institute, Central South University (Changsha, China). All animal experimental protocols
27
28 were evaluated and approved by the Ethics Committee of Central South University. Both
29
30 genders of ICR mice (7 weeks, SLACCAS) were randomized and treated
31
32 intraperitoneally (ip) with a single dose of **10d** at 200, 250, 300, 350, 400, and 450 mg/kg,
33
34 respectively. Each group contained 10 animals and the animals were observed for
35
36 abnormal behavior and mortality up to two weeks post treatment.
37
38
39
40
41

42 Both genders of athymic BALB/c nude mice (4-5 weeks, SLACCAS) were inoculated
43
44 subcutaneously with A549/DDP cells (1×10^7 /mouse). After the solid tumors were
45
46 established and allowed to reach 180-200 mm³, the mice were randomized and treated
47
48 intraperitoneally with **10d** (20 mg/kg or 40 mg/kg) or the same volume of vehicle
49
50 consisting of PBS/DMSO/cremophor-EL (8:1:1) daily for 15 consecutive days. The
51
52 tumor growth was recorded every three days from the measurement of length and width
53
54
55
56
57
58
59
60

1
2
3
4 using a vernier caliper and calculated as Tumor volumes (TV) with the following formula:

5
6
7 $TV (mm^3) = Width^2 (Length/2)$. The tumor growth inhibition rate (weight per unit weight,
8
9 w/w, %) was calculated as described previously.⁵⁷
10

11 12 13 14 15 16 ASSOCIATED CONTENT

17
18
19 **Supporting Information.** The purities of compounds **10a-u**, IR spectra, ¹H and ¹³C
20
21 NMR spectra, MS and HRMS spectra of compounds **10a-u**, chemical characterization of
22
23 compound **9e**. This material is available free of charge via the Internet at
24
25 <http://pubs.acs.org>.
26
27
28
29

30 31 32 33 AUTHOR INFORMATION

34
35
36
37 **Corresponding Authors:** *Tel: +86-731-84805451, Fax: +86-731-84805451, E-mail:
38
39 rencaiping@csu.edu.cn (C. Ren); *Tel: +86-25-83271072, E-mail,
40
41 cpudahuang@163.com (Z. Huang); *Tel: +86-25-83271015, Fax: +86-25-83271015,
42
43 E-mail: zyhtgd@163.com (Y. Zhang).
44
45
46

47 **Author Contributions:** ‡Y.A. and B.Z. contributed equally to this work.
48
49

50 51 52 53 ACKNOWLEDGEMENTS

54
55
56 This study was supported by grants from the National Natural Science Foundation of
57
58
59
60

1
2
3
4 China (No. 81273378, No. 81202408, and No. 81272972), the National Basic Research
5
6
7 Program of China (2010CB833605), and Open-End Fund for the Valuable and Precision
8
9
10 Instruments of Central South University.

11 12 13 14 15 **ABBREVIATIONS USED**

16
17
18 AKT, a serine/threonine-protein kinase; DMSO, dimethyl sulfoxide; ERK, extracellular
19
20 regulated kinase; ESI, electrospray ionization; MTT, 3-[4,5-dimethyl-thiazol-2-yl]-2,5-
21
22 diphenyltetrazolium bromide; NADPH, nicotinamide adenine dinucleotide phosphate;
23
24
25
26 DTNB, 5,5'-dithiobis(2-nitrobenzoic) acid.
27
28
29
30
31
32
33
34
35
36
37
38

39 40 **REFERENCES**

- 41
42 (1) Waris, G.; Ahsan, H. Reactive oxygen species: role in the development of cancer and
43
44 various chronic conditions. *J. Carcinog.* **2006**, *5*, 14.
45
46
47 (2) Wu, W. S. The signaling mechanism of ROS in tumor progression. *Cancer Metastasis*
48
49 *Rev.* **2006**, *25*, 695-705.
50
51
52
53 (3) Gorrini, C.; Harris, I. S.; Mak, T. W. Modulation of oxidative stress as an anticancer
54
55 strategy. *Nat. Rev. Drug Discovery* **2013**, *12*, 931-947.
56
57
58
59
60

- 1
2
3
4 (4) Pelicano, H.; Carney, D.; Huang, P. ROS stress in cancer cells and therapeutic
5 implications. *Drug Resist. Updates* **2004**, *7*, 97-110.
6
7
8
9 (5) Deavall, D. G.; Martin, E. A.; Horner, J. M.; Roberts, R. Druginduced oxidative stress
10 and toxicity. *J. Toxicol.* **2012**, *2012*, 645460.
11
12
13 (6) Fang, J.; Seki, T.; Maeda, H. Therapeutic strategies by modulating oxygen stress in
14 cancer and inflammation. *Adv. Drug Deliv. Rev.* **2009**, *61*, 290-302.
15
16
17 (7) Raj, L.; Ide, T.; Gurkar, A. U.; Foley, M.; Schenone, M.; Li, X.; Tolliday, N. J.; Golub,
18 T. R.; Carr, S. A.; Shamji, A. F.; Stern, A. M.; Mandinova, A.; Schreiber, S. L.; Lee,
19 S. W. Selective killing of cancer cells by a small molecule targeting the stress
20 response to ROS. *Nature.* **2011**, *475*, 231-234.
21
22
23 (8) Huang, G.; Chen, H.; Dong, Y.; Luo, X.; Yu, H.; Moore, Z.; Bey, E. A.; Boothman, D.
24 A.; Gao, J. Superparamagnetic iron oxide nanoparticles: amplifying ROS stress to
25 improve anticancer drug efficacy. *Theranostics.* **2013**, *3*, 116-126.
26
27
28 (9) Yi, B.; Liu, D.; He, M.; Li, Q.; Liu, T.; Shao, J. Role of the ROS/AMPK signaling
29 pathway in tetramethylpyrazine-induced apoptosis in gastric cancer cells. *Oncol.*
30 *Lett.* **2013**, *6*, 583-589.
31
32
33 (10) Pelicano, H.; Feng, L.; Zhou, Y.; Carew, J. S.; Hileman, E. O.; Plunkett, W.; Keating,
34 M. J.; Huang, P. Inhibition of mitochondrial respiration: a novel strategy to enhance
35 drug-induced apoptosis in human leukemia cells by a reactive oxygen
36 species-mediated mechanism. *J. Biol. Chem.* **2003**, *278*, 37832-37839.
37
38
39 (11) Miller, W. H. Jr.; Schipper, H. M.; Lee, J. S.; Singer, J.; Waxman, S. Mechanisms of
40
41
42
43
44
45
46
47
48
49
50
51
52
53
54
55
56
57
58
59
60

1
2
3
4 action of arsenic trioxide. *Cancer Res.* **2002**, *62*, 3893-3903.

5
6
7 (12) Liu, Q.; Shuhendler, A.; Cheng, J.; Rauth, A. M.; O'Brien, P.; Wu, X. Y. Cytotoxicity
8
9 and mechanism of action of a new ROS-generating microsphere formulation for
10
11 circumventing multidrug resistance in breast cancer cells. *Breast Cancer Res. Treat.*
12
13 **2010**, *121*, 323-333.

14
15
16
17 (13) Cheng, J.; Liu, Q.; Shuhendler, A. J.; Rauth, A. M.; Wu, X. Y. Optimizing the design
18
19 and in vitro evaluation of bioreactive glucose oxidase-microspheres for enhanced
20
21 cytotoxicity against multidrug resistant breast cancer cells. *Colloids Surf. B*
22
23 *Biointerfaces.* **2015**, *130*, 164-172.

24
25
26
27 (14) Guo, S. K.; Chen, K. J.; Qian, Z. H.; Weng, W. L.; Qian, M. Y. Tetramethylpyrazine
28
29 in the treatment of cardiovascular and cerebrovascular diseases. *Planta Med.* **1983**,
30
31 *47*, 89.

32
33
34
35 (15) Yu, K.; Chen, Z.; Pan, X.; Yang, Y.; Tian, S.; Zhang, J.; Ge, J.; Ambati, B.; Zhuang, J.
36
37 Tetramethylpyrazine-mediated suppression of C6 gliomas involves inhibition of
38
39 chemokine receptor CXCR4 expression. *Oncol. Rep.* **2012**, *28*, 955-960.

40
41
42 (16) Zheng, C. Y.; Xiao, W.; Zhu, M. X.; Pan, X. J.; Yang, Z. H.; Zhou, S. Y. Inhibition of
43
44 cyclooxygenase-2 by tetramethylpyrazine and its effects on A549 cell invasion and
45
46 metastasis. *Int. J. Oncol.* **2012**, *40*, 2029-2037.

47
48
49 (17) Zhang, Y.; Liu, X.; Zuo, T.; Liu, Y.; Zhang, J. H. Tetramethylpyrazine reverses
50
51 multidrug resistance in breast cancer cells through regulating the expression and
52
53 function of P-glycoprotein. *Med. Oncol.* **2012**, *29*, 534-538.

- 1
2
3
4 (18) Wang, X. B.; Wang, S. S.; Zhang, Q. F.; Liu, M.; Li, H. L.; Liu, Y.; Wang, J. N.;
5
6 Zheng, F.; Guo, L. Y.; Xiang, J. Z. Inhibition of tetramethylpyrazine on P-gp, MRP2,
7
8 MRP3 and MRP5 in multidrug resistant human hepatocellular carcinoma cells.
9
10 *Oncol. Rep.* **2010**, *23*, 211-215.
11
12
13
14 (19) Cheng, X. C.; Liu, X. Y.; Xu, W. F.; Guo, X. L.; Zhang, N.; Song, Y. N. Ligustrazine
15
16 derivatives. Part 3: Design, synthesis and evaluation of novel acylpiperazinyl
17
18 derivatives as potential cerebrocardiac vascular agents. *Bioorg. Med. Chem.* **2009**,
19
20 *17*, 3018-3024.
21
22
23
24 (20) Fang, J.; Sawa, T.; Akaike, T.; Akuta, T.; Sahoo, S. K.; Khaled, G.; Hamada, A.;
25
26 Maeda, H. In vivo antitumor activity of pegylated zinc protoporphyrin: targeted
27
28 inhibition of heme oxygenase in solid tumor. *Cancer Res.* **2003**, *63*, 3567-3574.
29
30
31
32 (21) Maeda, H.; Hori, S.; Ohizumi, H.; Segawa, T.; Kakehi, Y.; Ogawa, O.; Kakizuka, A.
33
34 Effective treatment of advanced solid tumors by the combination of arsenic trioxide
35
36 and L-buthionine-sulfoximine. *Cell Death Differ.* **2004**, *11*, 737-746.
37
38
39
40 (22) Trachootham, D.; Zhou, Y.; Zhang, H.; Demizu, Y.; Chen, Z.; Pelicano, H.; Chiao,
41
42 P.J.; Achanta, G.; Arlinghaus, R. B.; Liu, J.; Huang, P. Selective killing of
43
44 oncogenically transformed cells through a ROS-mediated mechanism by
45
46 beta-phenylethyl isothiocyanate. *Cancer Cell.* **2006**, *10*, 241-252.
47
48
49
50 (23) Lu, J.; Holmgren, A. The thioredoxin antioxidant system. *Free Radical Biol. Med.*
51
52
53
54 **2014**, *66*, 75-87.
55
56
57 (24) Mahmood, D. F.; Abderrazak, A.; Khadija, E. H.; Simmet, T.; Rouis, M. The
58
59
60

1
2
3
4 thioredoxin system as a therapeutic target in human health and disease. *Antioxid.*
5
6
7 *Redox Signaling* **2013**, *19*, 1266-1303.

8
9
10 (25) Bindoli, A.; Rigobello, M. P. Principles in redox signaling: from chemistry to
11
12 functional significance. *Antioxid. Redox Signaling* **2013**, *18*, 1557-1593.

13
14 (26) Kahlos, K.; Soini, Y.; Saily, M.; Koistinen, P.; Kakko, S.; Paakko, P.; Holmgren, A.;
15
16 Kinnula, V. L. Up-regulation of thioredoxin and thioredoxin reductase in human
17
18 malignant pleural mesothelioma. *Int. J. Cancer* **2001**, *95*, 198-204.

19
20
21 (27) Berggren, M.; Gallegos, A.; Gasdaska, J. R.; Gasdaska, P. Y.; Warneke, J.; Powis, G.
22
23 Thioredoxin and thioredoxin reductase gene expression in human tumors and cell
24
25 lines, and the effects of serum stimulation and hypoxia. *Anticancer Res.* **1996**, *16*,
26
27 3459-3466.

28
29 (28) Kim, S. J.; Miyoshi, Y.; Taguchi, T.; Tamaki, Y.; Nakamura, H.; Yodoi, J.; Kato, K.;
30
31 Noguchi, S. High thioredoxin expression is associated with resistance to docetaxel
32
33 in primary breast cancer. *Clin. Cancer Res.* **2005**, *11*, 8425-8430.

34
35 (29) Trachootham, D.; Alexandre, J.; Huang, P. Targeting cancer cells by ROS-mediated
36
37 mechanisms: a radical therapeutic approach? *Nat. Rev. Drug Discovery* **2009**, *8*,
38
39 579-591.

40
41 (30) Cai, W.; Zhang, L.; Song, Y.; Wang, B.; Zhang, B.; Cui, X.; Hu, G.; Liu, Y.; Wu, J.;
42
43 Fang, J. Small molecule inhibitors of mammalian thioredoxin reductase. *Free*
44
45 *Radical Biol. Med.* **2012**, *52*, 257-265.

46
47
48 (31) Liu, Y.; Li, Y.; Yu, S.; Zhao, G. Recent advances in the development of thioredoxin
49
50
51
52
53
54
55
56
57
58
59
60

- 1
2
3
4 reductase inhibitors as anticancer agents. *Curr. Drug Targets.* **2012**, *13*, 1432-1444.
- 5
6
7 (32) Zou, T.; Lum, C. T.; Lok, C. N.; To, W. P.; Low, K. H.; Che, C. M. A binuclear gold(I)
8
9 complex with mixed bridging diphosphine and bis(N-heterocyclic carbene) ligands
10
11 shows favorable thiol reactivity and inhibits tumor growth and angiogenesis in vivo.
12
13 *Angew. Chem., Int. Ed.* **2014**, *53*, 5810-5814.
- 14
15
16
17 (33) Zhang, D.; Xu, Z.; Yuan, J.; Zhao, Y. X.; Qiao, Z. Y.; Gao, Y. J.; Yu, G. A.; Li, J.;
18
19 Wang, H. Synthesis and molecular recognition studies on small-molecule inhibitors
20
21 for thioredoxin reductase. *J. Med. Chem.* **2014**, *57*, 8132-8139.
- 22
23
24
25 (34) Liu, Y.; Duan, D.; Yao, J.; Zhang, B.; Peng, S.; Ma, H.; Song, Y.; Fang, J.
26
27 Dithiaarsanes induce oxidative stress-mediated apoptosis in HL-60 cells by
28
29 selectively targeting thioredoxin reductase. *J. Med. Chem.* **2014**, *57*, 5203-5211.
- 30
31
32
33 (35) Huang, L.; Chen, Y.; Liang, B.; Xing, B.; Wen, G.; Wang, S.; Yue, X.; Zhu, C.; Du, J.;
34
35 Bu, X. A furanyl acryl conjugated coumarin as an efficient inhibitor and a highly
36
37 selective off-on fluorescent probe for covalent labelling of thioredoxin reductase.
38
39 *Chem. Commun.* **2014**, *50*, 6987-6990.
- 40
41
42
43 (36) Citta, A.; Folda, A.; Bindoli, A.; Pigeon, P.; Top, S.; Vessieres, A.; Salmain, M.;
44
45 Jaouen, G.; Rigobello, M. P. Evidence for targeting thioredoxin reductases with
46
47 ferrocenyl quinone methides. A possible molecular basis for the antiproliferative
48
49 effect of hydroxyferrocifens on cancer cells. *J. Med. Chem.* **2014**, *57*, 8849-8859.
- 50
51
52
53 (37) Zhang, B.; Duan, D.; Ge, C.; Yao, J.; Liu, Y.; Li, X.; Fang, J. Synthesis of
54
55 xanthohumol analogues and discovery of potent thioredoxin reductase inhibitor as
56
57
58
59

- 1
2
3
4 potential anticancer agent. *J. Med. Chem.* **2015**, *58*, 1795-1805.
5
6
7 (38) Maheshwari, R. K.; Singh, A. K.; Gaddipati, J.; Srimal, R. C.; Multiple biological
8
9 activities of curcumin: a short review. *Life Sci.* **2006**, *78*, 2081-2087.
10
11
12 (39) Gafner, S.; Lee, S. K.; Cuendet, M.; Barthélémy, S.; Vergnes, L.; Labidalle, S.;
13
14 Mehta, R. G.; Boone, C. W.; Pezzuto, J. M. Biologic evaluation of curcumin and
15
16 structural derivatives in cancer chemoprevention model systems. *Phytochemistry.*
17
18
19 **2004**, *65*, 2849-2859.
20
21
22 (40) Qiu, X.; Liu, Z.; Shao, W. Y.; Liu, X.; Jing, D. P.; Yu, Y. J.; An, L. K.; Huang, S. L.;
23
24 Bu, X. Z.; Huang, Z. S.; Gu, L. Q. Synthesis and evaluation of curcumin analogues
25
26 as potential thioredoxin reductase inhibitors. *Bioorg. Med. Chem.* **2008**, *16*,
27
28
29 8035-8041.
30
31
32 (41) Zhou, B.; Huang, J.; Zuo, Y.; Li, B.; Guo, Q.; Cui, B.; Shao, W.; Du, J.; Bu, X. 2a, a
33
34 novel curcumin analog, sensitizes cisplatin-resistant A549 cells to cisplatin by
35
36 inhibiting thioredoxin reductase concomitant oxidative stress damage. *Eur. J.*
37
38
39 *Pharmacol.* **2013**, *707*, 130-139.
40
41
42 (42) Adams, B. K.; Ferstl, E. M.; Davis, M. C.; Herold, M.; Kurtkaya, S.; Camalier, R. F.;
43
44 Hollingshead, M. G.; Kaur, G.; Sausville, E. A.; Rickles, F. R.; Snyder, J. P.; Liotta,
45
46
47 D. C.; Shoji, M. Synthesis and biological evaluation of novel curcumin analogs as
48
49
50 anticancer and antiangiogenesis agents. *Bioorg. Med. Chem.* **2004**, *12*, 3871-3883.
51
52
53 (43) Wang, Y.; Xiao, J.; Zhou, H.; Yang, S.; Wu, X.; Jiang, C.; Zhao, Y.; Liang, D.; Li, X.;
54
55
56 Liang, G. A novel monocarbonyl analogue of curcumin,
57
58
59

- 1
2
3
4 (1E,4E)-1,5-bis(2,3-dimethoxyphenyl)penta-1,4-dien-3-one, induced cancer cell
5
6
7 H460 apoptosis via activation of endoplasmic reticulum stress signaling pathway. *J.*
8
9
10 *Med. Chem.* **2011**, *54*, 3768-3778.
- 11
12 (44) Wang, R.; Chen, C.; Zhang, X.; Zhang, C.; Zhong, Q.; Chen, G.; Zhang, Q.; Zheng,
13
14 S.; Wang, G.; Chen, Q. H. Structure-activity relationship and pharmacokinetic
15
16 studies of 1,5-diheteroaryl penta-1,4-dien-3-ones: A class of promising
17
18 curcumin-based anti-cancer agents. *J. Med. Chem.* **2015**, *58*, 4713-4726.
- 19
20
21
22 (45) Subramaniam, D.; May, R.; Sureban, S. M.; Lee, K. B.; George, R.; Kuppusamy, P.;
23
24 Ramanujam, R. P.; Hideg, K.; Dieckgraefe, B. K.; Houchen, C. W.; Anant, S.
25
26 Diphenyl difluoroketone: a curcumin derivative with potent in vivo anticancer
27
28 activity. *Cancer Res.* **2008**, *68*, 1962-1969.
- 29
30
31
32 (46) Liang, Y.; Yin, D.; Hou, L.; Zheng, T.; Wang, J.; Meng, X.; Lu, Z.; Song, X.; Pan, S.;
33
34 Jiang, H.; Liu, L. Diphenyl difluoroketone: a potent chemotherapy candidate for
35
36 human hepatocellular carcinoma. *PLoS One.* **2011**, *6*, e23908.
- 37
38
39
40 (47) Liu, H.; Liang, Y.; Wang, L.; Tian, L.; Song, R.; Han, T.; Pan, S.; Liu, L. In vivo and
41
42 in vitro suppression of hepatocellular carcinoma by EF24, a curcumin analog. *PLoS*
43
44 *One.* **2012**, *7*, e48075.
- 45
46
47
48 (48) Nagaraju, G. P.; Zhu, S.; Wen, J.; Farris, A. B.; Adsay, V. N.; Diaz, R.; Snyder, J. P.;
49
50 Mamoru, S.; El-Rayes, B. F. Novel synthetic curcumin analogues EF31 and UBS109
51
52 are potent DNA hypomethylating agents in pancreatic cancer. *Cancer Lett.* **2013**,
53
54 *341*, 195-203.

- 1
2
3
4 (49) Nagaraju, G. P.; Zhu, S.; Ko, J. E.; Ashritha, N.; Kandimalla, R.; Snyder, J. P.; Shoji,
5
6 M.; El-Rayes, B. F. Antiangiogenic effects of a novel synthetic curcumin analogue in
7
8 pancreatic cancer. *Cancer Lett.* **2015**, *357*, 557-565.
9
10
11
12 (50) Brown, A.; Shi, Q.; Moore, T. W.; Yoon, Y.; Prussia, A.; Maddox, C.; Liotta, D. C.;
13
14 Shim, H.; Snyder, J. P. Monocarbonyl curcumin analogues: heterocyclic pleiotropic
15
16 kinase inhibitors that mediate anticancer properties. *J. Med. Chem.* **2013**, *56*,
17
18 3456-3466.
19
20
21
22 (51) Kimani, S. G.; Phillips, J. B.; Bruce, J. I.; MacRobert, A. J.; Golding, J. P.
23
24 Antioxidant inhibitors potentiate the cytotoxicity of photodynamic therapy.
25
26 *Photochem. Photobiol.* **2012**, *88*, 175-187.
27
28
29
30 (52) Cheng, X. C.; Liu, X. Y.; Xu, W. F.; Guo, X. L.; Ou, Y. Design, synthesis, and
31
32 biological activities of novel Ligustrazine derivatives. *Bioorg. Med. Chem.* **2007**, *15*,
33
34 3315-3320.
35
36
37
38 (53) Zumbansen, K.; Döhning, A.; List, B. Morpholinium trifluoroacetate-catalyzed aldol
39
40 condensation of acetone with both aromatic and aliphatic aldehydes. *Adv. Synth.*
41
42 *Catal.* **2010**, *352*, 1135-1138.
43
44
45
46 (54) Steinbrenner, H.; Sies, H. Protection against reactive oxygen species by
47
48 selenoproteins. *Biochim. Biophys. Acta.* **2009**, *1790*, 1478-1485.
49
50
51
52 (55) Esatbeyoglu, T.; Huebbe, P.; Ernst, I. M.; Chin, D.; Wagner, A. E.; Rimbach, G.
53
54 Curcumin--from molecule to biological function. *Angew. Chem., Int. Ed.* **2012**, *51*,
55
56 5308-5332.
57
58
59
60

- 1
2
3
4 (56) Mi, Y.; Xiao, C.; Du, Q.; Wu, W.; Qi, G.; Liu, X. Momordin Ic couples apoptosis
5
6 with autophagy in human hepatoblastoma cancer cells by reactive oxygen species
7
8 (ROS)-mediated PI3K/Akt and MAPK signaling pathways. *Free Radic. Biol. Med.*
9
10 **2016**, *90*, 230-242.
11
12
13
14 (57) Ai, Y.; Kang, F.; Huang, Z.; Xue, X.; Lai, Y.; Peng, S.; Tian, J.; Zhang, Y. Synthesis
15
16 of CDDO-amino acid-nitric oxide donor trihybrids as potential antitumor agents
17
18 against both drug-sensitive and drug-resistant colon cancer. *J. Med. Chem.* **2015**, *58*,
19
20 2452-2464.
21
22
23
24 (58) Lin, X.; Zhang, X.; Wang, Q.; Li, J.; Zhang, P.; Zhao, M.; Li, X. Perifosine
25
26 downregulates MDR1 gene expression and reverses multidrug-resistant phenotype
27
28 by inhibiting PI3K/Akt/NF- κ B signaling pathway in a human breast cancer cell line.
29
30 *Neoplasma.* **2012**, *59*, 248-256.
31
32
33
34 (59) Kuo, M. T.; Liu, Z.; Wei, Y.; Lin-Lee, Y. C.; Tatebe, S.; Mills, G. B.; Unate, H.
35
36 Induction of human MDR1 gene expression by 2-acetylaminofluorene is mediated
37
38 by effectors of the phosphoinositide 3-kinase pathway that activate NF-kappaB
39
40 signaling. *Oncogene.* **2002**, *21*, 1945-1954.
41
42
43
44 (60) Qiu, X.; Du, Y.; Lou, B.; Zuo, Y.; Shao, W.; Huo, Y.; Huang, J.; Yu, Y.; Zhou, B.; Du,
45
46 J.; Fu, H.; Bu, X. Synthesis and identification of new 4-arylidene curcumin
47
48 analogues as potential anticancer agents targeting nuclear factor- κ B signaling
49
50 pathway. *J. Med. Chem.* **2010**, *53*, 8260-8273.
51
52
53
54 (61) Tsubaki, M.; Takeda, T.; Ogawa, N.; Sakamoto, K.; Shimaoka, H.; Fujita, A.; Itoh, T.;
55
56 Imano, M.; Ishizaka, T.; Satou, T.; Nishida, S. Overexpression of survivin via
57
58
59
60

- 1
2
3 activation of ERK1/2, Akt, and NF- κ B plays a central role in vincristine resistance
4
5 in multiple myeloma cells. *Leuk. Res.* **2015**, *39*, 445-452.
6
7
8 (62) Xi, G.; Hayes, E.; Lewis, R.; Ichi, S.; Mania-Farnell, B.; Shim, K.; Takao, T.;
9
10 Allender, E.; Mayanil, C. S.; Tomita, T. CD133 and DNA-PK regulate MDR1 via
11
12 the PI3K- or Akt-NF- κ B pathway in multidrug-resistant glioblastoma cells in vitro.
13
14 *Oncogene.* **2016**, *35*, 241-250.
15
16
17 (63) Dolado, I.; Nebreda, A. R. AKT and oxidative stress team up to kill cancer cells.
18
19 *Cancer Cell.* **2008**, *14*, 427-429.
20
21
22 (64) Colabufo, N. A.; Berardi, F.; Cantore, M.; Contino, M.; Inglese, C.; Niso, M.;
23
24 Perrone, R. Perspectives of P-glycoprotein modulating agents in oncology and
25
26 neurodegenerative diseases: pharmaceutical, biological, and diagnostic potentials. *J.*
27
28 *Med. Chem.* **2010**, *53*, 1883-1897.
29
30
31 (65) Hitchcock, S. A. Structural modifications that alter the P-glycoprotein efflux
32
33 properties of compounds. *J. Med. Chem.* **2012**, *55*, 4877-4895.
34
35
36
37 (66) Li, S.; Zhang, W.; Yin, X.; Xing, S.; Xie, H.Q.; Cao, Z.; Zhao, B. Mouse
38
39 ATP-binding cassette (ABC) transporters conferring multi-drug resistance.
40
41 *Anticancer Agents Med. Chem.* **2015**, *15*, 423-432.
42
43
44
45 (67) Gillet, J. P.; Gottesman, M. M. Mechanisms of multidrug resistance in cancer.
46
47 *Methods Mol. Biol.* **2010**, *596*, 47-76.
48
49
50 (68) Choi, Y. H.; Yu, A. M. ABC transporters in multidrug resistance and
51
52 pharmacokinetics, and strategies for drug development. *Curr. Pharm. Des.* **2014**, *20*,
53
54 793-807.
55
56
57
58
59
60

- 1
2
3
4 (69) Shukla, S.; Ohnuma, S.; Ambudkar, S. V. Improving cancer chemotherapy with
5
6 modulators of ABC drug transporters. *Curr. Drug Targets*. **2011**, *12*, 621-630.
7
8 (70) Holohan, C.; Van Schaeybroeck, S.; Longley, D. B.; Johnston, P. G. Cancer drug
9
10 resistance: an evolving paradigm. *Nat. Rev. Cancer*. **2013**, *13*, 714-726.
11
12 (71) Eckford, P. D.; Sharom, F. J. ABC efflux pump-based resistance to chemotherapy
13
14 drugs. *Chem. Rev.* **2009**, *109*, 2989-3011.
15
16
17 (72) Wang, Y. M.; Hu, L. X.; Liu, Z. M.; You, X. F.; Zhang, S. H.; Qu, J. R.; Li, Z. R.; Li,
18
19 Y.; Kong, W. J.; He, H. W.; Shao, R. G.; Zhang, L. R.; Peng, Z. G.; Boykin, D. W.;
20
21 Jiang, J. D. N-(2,6-dimethoxypyridine-3-yl)-9-methylcarbazole-3-sulfonamide as a
22
23 novel tubulin ligand against human cancer. *Clin. Cancer Res.* **2008**, *14*, 6218-6227.
24
25
26 (73) Kim, M. K.; Choo, H.; Chong, Y. Water-soluble and cleavable quercetin-amino acid
27
28 conjugates as safe modulators for P-glycoprotein-based multidrug resistance. *J. Med.*
29
30 *Chem.* **2014**, *57*, 7216-7233.
31
32
33 (74) Chen, W.; Chen, H.; Xiao, F.; Deng, G. J. Palladium-catalyzed conjugate addition of
34
35 arylsulfonyl hydrazides to α,β -unsaturated ketones. *Org. Biomol. Chem.* **2013**, *11*,
36
37 4295-4298.
38
39
40 (75) Chuprajob, T.; Changtam, C.; Chokchaisiri, R.; Chunglok, W.; Nilubon Sornkaew,
41
42 N.; Suksamrarn, A. Synthesis, cytotoxicity against human oral cancer KB cells and
43
44 structure-activity relationship studies of trienone analogues of curcuminoids. *Bioorg.*
45
46 *Med. Chem. Lett.* **2014**, *24*, 2839-2844.
47
48
49 (76) Leung, P. S. W.; Teng, Y.; Toy, P. H. Chromatography-free Wittig reactions using a
50
51 bifunctional polymeric reagent. *Org. Lett.* **2010**, *12*, 4996-4999.
52
53
54 (77) Ning, X.; Guo, Y.; Ma, X.; Zhu, R.; Tian, C.; Wang, X.; Ma, Z.; Zhang, Z.; Liu, J.
55
56
57
58
59
60

1
2
3 Synthesis and neuroprotective effect of E-3,4-dihydroxy styryl aralkyl ketones
4 derivatives against oxidative stress and inflammation. *Bioorg. Med. Chem. Lett.*
5
6
7
8 **2013**, *23*, 3700-3703.
9

10 (78) Zhang, W.; Benmohamed, R.; Arvanites, A. C.; Morimoto, R. I.; Robert J. Ferrante,
11 R. J.; Kirsch, D. R.; Silverman, R. B. Cyclohexane 1,3-diones and their inhibition of
12 mutant SOD1-dependent protein aggregation and toxicity in PC12 cells. *Bioorgan.*
13
14
15
16
17
18
19 *Med. Chem.* **2012**, *20*, 1029-1045.

20 (79) Lin, Y. M.; Li, Z.; Casarotto, V.; Ehrmantraut, J.; Nguyen, A. N. A catalytic, highly
21 stereoselective aldehyde olefination reaction. *Tetrahedron Lett.* **2007**, *48*,
22
23
24
25
26
27
28
29
30
31
32
33
34
35
36
37
38
39
40
41
42
43
44
45
46
47
48
49
50
51
52
53
54
55
56
57
58
59
60
5531-5534.

(80) Xie, Q.; Lan, G.; Zhou, Y.; Huang, J.; Liang, Y.; Zheng, W.; Fu, X.; Fan, C.; Chen,
T. Strategy to enhance the anticancer efficacy of X-ray radiotherapy in melanoma
cells by platinum complexes, the role of ROS-mediated signaling pathways. *Cancer*
Lett. **2014**, *354*, 58-67.

(81) Dai, C.; Tiwari, A. K.; Wu, C. P.; Su, X.; Wang, S. R.; Liu, D.; Ashby, C. R.; Huang,
Y.; Robey, R. W.; Liang, Y. Lapatinib (Tykerb, GW572016) reverses multidrug
resistance in cancer cells by inhibiting the activity of ATP-binding cassette
subfamily B member 1 and G member 2. *Cancer Res.* **2008**, *68*, 7905-7914.

(82) Zhang, D. M.; Shu, C.; Chen, J. J.; Sodani, K.; Wang, J.; Bhatnagar, J.; Lan, P.; Ruan,
Z. X.; Xiao, Z. J.; Ambudkar, S. V.; Chen, W. M.; Chen, Z. S.; Ye, W. C. BBA, a
derivative of 23-hydroxybetulinic acid, potently reverses ABCB1-mediated drug
resistance in vitro and in vivo. *Mol. Pharm.* **2012**, *9*, 3147-3159.

1
2
3
4
5
6
7
8
9
10
11
12
13
14
15
16
17
18
19
20
21
22
23
24
25
26
27
28
29
30
31
32
33
34
35
36
37
38
39
40
41
42
43
44
45
46
47
48
49
50
51
52
53
54
55
56
57
58
59
60

Table of Contents Graphic

